Base Catalysis by Alkali Modified Zeolites

by

Paul Edward Hathaway

Dissertation submitted to the Faculty of the

Virginia Polytechnic Institute and State University

in partial fulfillment of the requirements for the degree of

Doctor of Philosophy

in

Chemical Engineering

APPROVED:

Mark E. Davis, Chairman

David F. Cox

Brian E. Hanson

Joseph S. Merola

Felix Sebba

March, 1989

Blacksburg, Virginia

Base Catalysis by Alkali Modified Zeolites

by

Paul Edward Hathaway

Mark E. Davis, Chairman

Chemical Engineering

(ABSTRACT)

The development, characterization, and catalytic application of a novel zeolite with solid base properties has been completed. From isopropanol decomposition to acetone and propylene, the acid/base properties of various alkali exchanged, faujasite-type zeolites are explored. It is found that upon impregnation of CsNaY with cesium hydroxide or cesium acetate, acetone production (normally attributed to base sites) is promoted by an order of magnitude above the untreated (not impregnated) CsNaY zeolite. Furthermore, selectivity to acetone is above 97% and on a surface area basis, acetone activity is found to be comparable to MgO. Impregnation of CsNaX shows little promotion in acetone activity resulting in acetone activity comparable to the untreated CsNaY zeolite and acetone selectivity at 62%. From numerous characterization studies of the impregnated CsNaY zeolite (many *in situ*) it appears that a highly dispersed , intracrystalline cesium oxide is formed from the decomposition of the occluded salt and is believed to be the active site for acetone formation. Evidence is provided also to indicate the presence of an isopropoxide intermediate which is responsible for the acetone and the minor amounts of propylene formed by the acetate impregnated CsNaY zeolite.

The cesium acetate impregnated CsNaY catalyst was tested for activity by the base catalyzed alkylation of toluene, acetone, ethane, and methane with methanol. For toluene alkylation, it is determined that little improvement is gained over previous

faujasite-type catalysts. This appears to be a result of the rapid decomposition of formaldehyde, i.e., the alkylating agent derived from the dehydrogenation of methanol. MgO is demonstated to possess base properties similar to the acetate impregnated CsNaY zeolite, yet MgO is found to be inactive in toluene alkylation. Neither ethane or methane is alkylated at 425°C or 465°C by the acetate impregnated zeolites. Acetone is alkylated slightly to methylvinylketone and methylethylketone at 425°C but the majority of the reacted acetone appears to form aldol condensation products.

Acknowledgements

I wish to first thank Professor Mark Davis not only for his time and patience (How many times did I rewrite our first paper?) but for his complete trust in my results and conclusions. I sincerely feel that these attributes were essential to the success of this project and to our long standing friendship. I shall truely miss happy hour, volleyball, Columbian-poker, and pictionary.

I wish to thank the National Science Foundation, the Dow Chemical Company, the Cunningham Fellowship Committee, and the Pratt Presidential Fellowship Committee (i.e., Dr. Conger) for the financial support of this project.

I wish to thank the secretaries of the Chemical Engineering Deptartment (, , , and) for all their help in this project and others (e.g., keeping me enroled and locating my job).

I wish to thank Professor David Cox for giving me the opportunity to thrash him on the golf course.

I wish to thank for his friendship and all around good humor. He is truely the Einstein of fashion and the Vidal Sasoon of science.

I wish to thank (aye captain) for his good friendship during my last year. I truely wish he had arrived on the scene earlier.

On the domestic side, I wish to thank my family for their love and support. And lastly, I wish to expess a very special thanks to for her love and friendship.

To Mom and Dad

Table of Contents

List of Illustrations

List of Tables

Chapter 1

Introduction

In the development of zeolites as solid acid catalysts, it was found that zeolites inherently possess three important properties: (i) high Bronstëd acid strength, (ii) high surface area, and (iii) shape selectivity (both reactant/product and transition state selectivity). Although mixed oxides possess moderate acid strength and surface area, the tremendous potential of zeolites for acid catalysis comes from their inherent shape selective nature. Moreover, zeolite catalysts can be "designed" by (i) manipulation of crystal shape and size, (ii) the nature of the channel system, (iii) shape and size of the pores, and (iv) the nature and number of active sites. As a result of these properties, tremendous strides have been and continue to be made in acid catalysis by zeolites.

Solid base catalysts are typically oxides. Clearly, from the example set above the development of a basic zeolite could have tremendous implication in base catalysis. What follows here is the successful development, characterization and application of a novel zeolite catalyst with base properties.

Chapter 2

Catalytic Activity

2.1 Abstract

Isopropanol is reacted over alkali-exchanged X and Y zeolites in the presence and absence of occluded exchange salts at 350°C and atmospheric pressure. The decomposition of cesium acetate occluded in CsNaY results in the generation of a very active base site. This site improves the acetone activity of the parent CsNaY by an order of magnitude. The CsNaX zeolite, however, does not contain this site after decomposition of the occluded cesium acetate and as a result shows an acetone activity comparable to that observed for the parent CsNaY. For the cesium acetate occluded CsNaY zeolite, the selectivity to acetone is above 97%, and on a surface area basis, the acetone activity is comparable to that found for MgO.

2.2 *Introduction*

The use of alkali exchanged zeolites for base catalysis has received little attention, and even less attention has been directed towards the development and characterization of these sieves as solid bases. In characterizing these materials a technique for measuring both base strength and site distribution at reaction conditions would be ideal. However, no technique which combines these measurements is available (1).

Isopropanol decomposition has been employed to probe the acid and base properties of metal oxides at elevated temperatures (2). The assignment of the decomposition products to acid and base sites, however, deserves considerable caution. There is little question that over Bronstëd acid sites, alcohols can dehydrate to form olefins by an elimination mechanism (3). The problem, however, is the possible misinterpretation that olefin activity is only a result of Bronstëd acidity. It has been demonstrated that over metal oxides alcohols can dissociatively adsorb to form alkoxides (4-6). From the alkoxide intermediate, it has been suggested that dehydration or dehydrogenation can occur (7-12). Factors such as the structure (2,13) and electronic nature(8) of the oxide surface as well as the structure (7,11,12) and partial pressure (8) of the reacting alcohol have been shown to influence the pathway of the reacting alkoxide. As a result, no clear distinction can be made between the olefins formed over Bronstëd acid sites and those formed from the alkoxide decomposition. Furthermore, because of the many factors involved in the decomposition pathway of the alkoxide intermediate, it becomes increasingly difficult to know whether metal oxide catalysts which exhibit propylene activity will be effective in other base catalyzed reactions.

There appears to be agreement that with metal oxides dehydrogenation occurs over basic sites (4-12). It, therefore, seems plausible for isopropanol decomposition that

catalysts with high acetone activity and selectivity are likely to be effective in other base catalyzed reactions. Thus, by developing molecular sieves which exhibit high acetone activity and selectivity, we may expect that these sieves will be active in other base catalyzed reactions.

An investigation on the basic nature of alkali-exchanged X and Y zeolites by isopropanol decomposition was reported by Yashima et al. (14). In that study, zeolite Y was shown to be more selective to acetone formation than zeolite X. The selectivity to acetone, however, never exceeded 50% at conversions above 22%. Nagy et al. (15) studied the decomposition of isopropanol to characterize the acid/base nature of K^+ and Cs^+ exchanged ZSM-5. At identical conversions, Cs-ZSM-5 was found to be more selective to acetone formation at 60%. However, Derewinski et al. (16) observed mainly propylene and higher oligomers in the decomposition of isopropanol over alkali-exchanged ZSM-5.

The base properties of alkali-exchanged X and Y zeolites have been investigated also by Barthomeuf (17) who examined pyrrole adsorbed on the zeolites by infrared spectroscopy. The results suggested the following order in base strength: CsX > RbX > KX > NaX > RbY > KY.

Alkali-exchanged X and Y zeolites have been investigated extensively for the base catalyzed alkylation of toluene with methanol (18-20). From these studies, CsNaX is considered to be the most effective for side-chain alkylation over the other alkali-exchanged X and Y zeolites. The level of activity, however, appears to be the major obstacle in competing with present commercial processes.

Martens et al. (21) recently investigated large pore zeolites containing sodium clusters as base catalysts. From this study, it was suggested that framework oxygen anions in the neighborhood of intracrystalline neutral sodium clusters act as the active base site.

Base catalysis over alkali-exchanged molecular sieves is an area of growing interest. We have, therefore, systematically investigated the preparation and catalytic activity of alkali-exchanged X and Y zeolites in order to assess their ability to act as base catalysts.

2.3 Experimental

2.3.1 Materials

Zeolites X and Y were synthesized using the following gel compositions: $3.9Na_2O:Al_2O_3:3.0SiO_2:160H_2O$ and $2.4Na_2O:Al_2O_3:6.1SiO_2:95H_2O$, respectively. For zeolite X, the gel was aged 4 hours at 25°C and then heated for 13 hours at 100°C. In the case of zeolite Y, the gel was aged 48 hours at 25°C and then heated for 24 hours at 100°C. The X zeolite crystallized without extraneous impurities, but the Y zeolite contained considerable amounts of amorphous material. The amorphous material was separated from the Y zeolite by stirring the mixture in deionized water, allowing the crystalline material to settle to the bottom, and discarding the supernatant liquid. Zeolites X and Y prepared by this procedure were found to be highly crystalline from both X-ray diffraction and nitrogen adsorption (*vide infra*). Isopropanol (99.5%) and all alkali salts were obtained from Aldrich. Helium (99.995%), oxygen (99.5%), and carbon dioxide (99.8%) were obtained from AIRCO , and used with no further purification.

2.3.2 Exchange Procedure

Zeolites X and Y were exchanged at 25°C with 0.1N solutions of group 1A metal hydroxides. All catalysts were exchanged at 0.02 g/ml. The exchange procedure involved three exchanges which were performed for 24 hour time periods and a fourth exchange period which lasted 96 hours. After each exchange, the catalysts were filtered and re-slurried in fresh hydroxide solution. Upon completion of the 96 hour exchange, the catalysts were filtered and left unrinsed to prevent decationation (22). The catalysts were then placed in a convection oven to dry at 100°C.

Cesium hydroxide, acetate, nitrate, and chloride were each used to exchange Cs^+ into zeolite Y. The exchange and drying process were identical to that described above except that after the final filtration, half the filter cake was removed and left unrinsed, while the remaining half was rinsed with deionized water.

CsNaY was exchanged also in 0.3N and 0.5N solutions of cesium acetate and left unrinsed in an attempt to occlude higher quantities of cesium acetate.

The amount of cesium exchanged into zeolite Y was varied using the following technique. Solutions varying in alkali composition, i.e., XCsOH:(1-X)NaOH where $0 \leq X \leq 1$ were prepared such that the total alkali was fixed at 0.1N. The moles of CsOH in the solution were set by the desired loading of Cs^+ per unit cell. Again, the exchange was performed at 0.02g/ml. Only one exchange was performed which lasted 192 hours. From chemical analysis, it was determined that for lower loadings, e.g., ~8 Cs^+ per unit cell, nearly all the Cs^+ in the solution was exchanged. However, for higher loadings, some Cs^+ remained in the exchange solution.

2.3.3 Impregnation

Cesium acetate was impregnated into various supports using the following procedure. For a desired loading, a precalculated volume of a 0.025N cesium acetate solution, e.g., 3ml, was micropipetted into a vessel which contained the support. This mixture was then stirred overnight at ~40°C. The vessel was left open to air which allowed the water to slowly evaporate off. Using this procedure, a predicted 2.8wt% loading for silica gel and activated carbon yielded (from chemical analysis) a ~2.4wt% loading for both supports.

2.3.4 Analysis

Surface areas and pore volumes were determined by either nitrogen or oxygen adsorption on the Omnisorp 100 system developed by Omicron Technology.

Differential thermal analysis (DTA) was performed on a Dupont 900 Differential Thermal Analyzer. Most samples were heated in air. One sample, however, was analyzed in a helium atmosphere. An empty sample pan was used as a reference.

Infrared measurements were performed on an IBM IR/32 FTIR spectrometer which was equipped with a high temperature reaction cell similar to that reported by Hicks et al. (23). The window material was CaF_2 which is not infrared transparent below 1000 cm^{-1}.

Elemental analysis of the group 1A metal hydroxide exchanged zeolites was performed by Galbraith Laboratories, Inc. of Knoxville, TN. All other elemental analyses were performed in our laboratories by inductively coupled plasma or atomic absorption spectrometry.

Because of the many variables considered in the exchange of zeolite X and Y, a nomenclature was adopted. For example, consider CsNaY-OH-UR. Here, cesium was exchanged into zeolite Y, the exchange was performed from the hydroxide (OH), and the filter cake was left unrinsed (UR) after the final exchange. When necessary, the degree of ion exchange will be given,e.g., $Cs_{39}Na_{18}Y$-OH-UR.

2.3.5 Reactor System and Procedure

Isopropanol was pumped with a syringe pump into a 125°C constant temperature vaporizer where it was mixed with helium. This mixture could then bypass or feed into a vertical, down flow, fixed bed microreactor. The microreactor consisted of a 3mm I.D. vycor tube placed inside a tube furnace. Two start-up procedures were used and will be described in the following sections.

The zeolite catalysts were compacted without binder into pellets which were subsequently crushed and size separated. The resulting particles were -60/+80 mesh. Because the chemical composition differs for each catalyst, the weight per unit volume changes. For example, the CsNaX prepared here weighs 34% more than the NaX per unit volume. Therefore, the differences in rates between CsNaX and NaX on a gram basis could be misleading because there are less zeolite unit cells or supercages in a gram of CsNaX than in a gram of NaX. However, the number of supercages in a mole of CsNaX unit cells is equivalent to that found in a mole of NaX unit cells. Therefore, reaction rates have been normalized to a unit cell basis, i.e., moles of acetone or propylene formed per mole of zeolite unit cells per hour. Furthermore, because zeolite X and Y have identical crystal topologies, a direct comparison of activities between zeolite X and Y can be made on a unit cell basis.

The following conditions were found to give intrinsic reaction rate data: flow rates (STP) of helium and isopropanol were 180 ml min^{-1} and 45 ml min^{-1}, respectively, the reaction temperature was 350°C, and space velocities were above 6.7 mole isopropanol • (mole of zeolite unit cells) $^{-1}$ • sec^{-1}. Reaction products were analyzed by an on-line gas chromatograph which employed a Porapak T column (1/8" X 12') and a thermal conductivity detector. Response factors were measured and found to be in excellent agreement to those reported by Dietz (24).

2.4 Results and Discussion

2.4.1 Physical Properties

The composition, pore volume, and surface area of zeolite X and Y exchanged with the alkali hydroxides are given in Table 1. From bulk chemical analysis, the Si/Al ratio for zeolite X and Y is 1.34 and 2.34, respectively. The percent exchange was determined also and is listed for each catalyst. Because these catalysts were left unrinsed after the final filtration, an excess of alkali was detected for several catalysts and is listed in Table 1. The percent excess listed is defined as the number of excess M^+ per framework Al^{3+} times 100%. This calculation assumes all Na^+ atoms are balancing framework charge. From the Si/Al ratio, the percent exchanged, and the percent excess (assumed to exist as MOH), the molecular weight of the unit cell can be calculated and is listed in Table 1. Note that as Na^+ was exchanged by the heavier alkali metals the weight of the unit

Table 1. Physical Data of Zeolite Catalysts for Isopropanol Decomposition.

Catalyst	Si/Al	% Exchanged[a]	% Excess	Molecular Wt. Per Unit Cell	Volume ($Å^3$/supercage)[b]	BET Area (m^2/g)[c]
Na X	1.34	-	-	13330	927	875
KNa X	1.34	82	-	14350	889	785
RbNa X	1.34	68	-	16810	859	657
CsNa X	1.34	51	-	17870	781	550
Na Y	2.34	-	12	13060	943	900
KNa Y	2.34	93	23	14380	910	795
RbNa Y	2.34	71	15	16230	810	623
CsNa Y	2.34	63	-	16770	694	526

a) Based on a unit cell composition of: NaY: $Na_{58}Al_{58}Si_{134}O_{384}$
NaX: $Na_{82}Al_{82}Si_{110}O_{384}$

b) Calculated from nitrogen adsorption at 77 K and 300 torr.

c) BET surface areas calculated from nitrogen adsorption data.

cell increases. Thus, all reaction rates reported in this work are normalized to a unit cell basis unless specified otherwise.

Because of the high electron density associated with the Rb^+ and Cs^+ exchanged zeolites, X-ray powder diffraction was found to be ineffective for determining crystallinity. Therefore, the degree of crystallinity for each material was determined by measuring pore volumes and surface areas via nitrogen adsorption at 77 K. The pore volumes normalized to a gram basis for NaX and NaY are 0.34 and 0.35 ml/g, respectively. These values are in excellent agreement with 0.32 and 0.35 ml/g given by Breck (25) for NaX and NaY, respectively. The pore volumes listed in Table 1, however, are normalized to a supercage basis (8 supercages per unit cell) as opposed to a weight basis in order to account for the differences in molecular weight. Thus, differences in the volume of nitrogen adsorbed by each catalyst is a result only of changes in available pore volume. Note that as Na^+ is exchanged by larger cations, the volume per supercage decreases accordingly.

2.4.2 Influence of Start Up

Two start-up procedures were employed. Procedure 1, which was used for all reaction rate determinations, began by heating the catalyst in flowing helium (unless stated otherwise) to a specified calcination temperature, e.g., 550°C. After a 4 hour calcination, the temperature was decreased to 450°C and reactant flow initiated. The reaction was run for 30 minutes at 450°C. Next, the reaction temperature was lowered to 350°C and the system was allowed to reach steady state prior to rate measurements. Procedure 1 was found to ensure that the system maintained a steady state conversion to both acetone and propylene (*vide infra*). Procedure 2, which was used to study the transient

kinetic behavior of the system, involved the same calcination conditions as procedure 1, but the reaction temperature was lowered directly to 350°C before initiation of the reactant flow. The acetone activity obtained with procedure 1 was greater than that of procedure 2 by approximately 25% while the propylene activity showed little dependence on the start-up procedure. The cause of this difference in acetone activity is unknown at this time.

2.4.3 Intrinsic Rates

Rates were determined at differential conversions. By varying the contact time, the rate of isopropanol decomposition was found to be independent of conversion for conversions below 3.5%. To test whether the measured rates were limited by diffusion, a plot of the ln(rate) versus $1/T\ K^{-1}$ was constructed for the acetone and propylene activity of CsNaY-OH-UR and is shown in Figure 1. No curvature is observed for temperatures below 375°C for both acetone and propylene formation. Also, no curvature is observed when the gaseous flow rate was lowered (Fig. 1), thus excluding film diffusion limitations. From these data an activation energy can be determined for acetone and propylene formation over CsNaY-OH-UR. The activation energy for propylene formation is 24 kcals • mol^{-1} which is within the range reported by Jacobs et al. (26) for NaY. The activation energy of acetone formation is 37 kcals • mol^{-1}. A value of the activation energy for acetone formation over alkali-exchanged zeolites could not be found in the open literature. However, our value agrees well with the 37 kcals • mol^{-1} reported by Waugh et al. (10) for the formation of acetone over ZnO using a temperature programmed reaction.

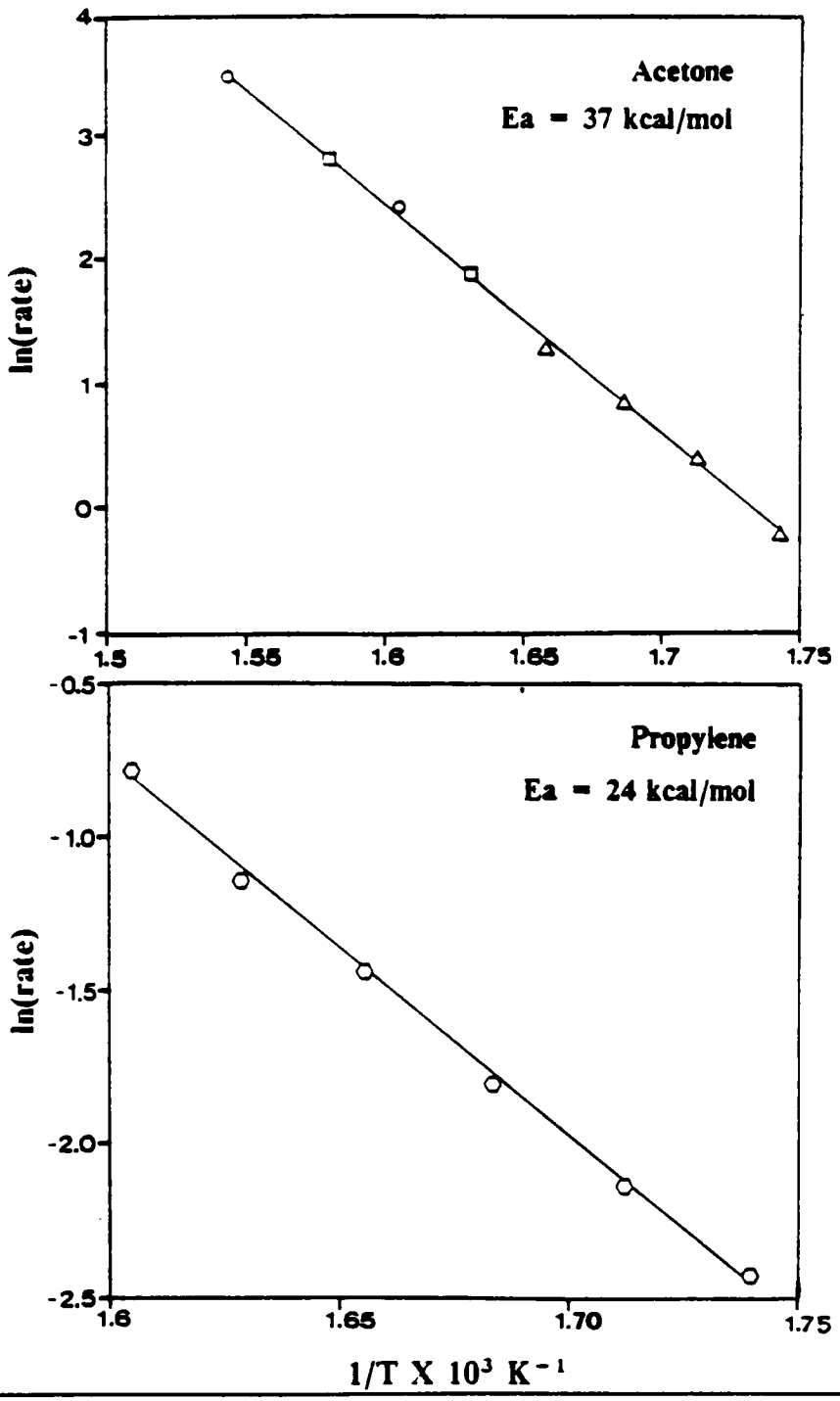

Figure 1 **Temperature Dependence of Acetone and Propylene Rates.** Acetone: ○ , F/W = 3.6 mol isopropanol • hr^{-1} • g^{-1}; □ , F/W = 3.6 mol isopropanol • hr^{-1} • g^{-1}; △ , F/W = 0.90 mol isopropanol•hr^{-1}•g^{-1}. Propylene: ⬡ , F/W = 0.90 mol isopropanol•hr^{-1}•g^{-1}. Total pressure = 1 atm., and partial pressure of isopropanol = 152 torr.

Table 2A lists the intrinsic rates of acetone and propylene formation of the hydroxide exchanged X and Y zeolites. NaX showed considerable propylene activity. Other than NaX, propylene formation, on a unit cell basis from the alkali-exchanged X zeolite catalysts was approximately twice that observed from the Y zeolite catalysts. The origin of propylene in alkali-exchanged zeolites is not fully understood. From infrared studies of pyridine adsorbed on NaX (27) and NaY (28), Ward concluded that there are no detectable Bronstëd or Lewis acid sites after calcining the materials at 500°C. However, Bronstëd acid sites were detected by pyridine adsorption on the alkaline earth forms of zeolite X and Y after a 500°C calcination. This is consistent with Mirodatos et al. (29,30) who showed from IR studies that water can interact with divalent cations of zeolite Y to form Bronstëd acid sites. Jacobs et al. (26) investigated isopropanol dehydration over alkali-exchanged X and Y zeolites and suggested that the observed activity could be a result of polyvalent cations at the impurity level reacting with water to form active acid sites. To investigate the possibility of divalent cations at the impurity level contributing to the propylene activity listed in Table 1A, ~8 Ca^{+2} per unit cell were exchanged into CsNaY-OH-UR. This material was then calcined at 550°C prior to the initiation of the reactant flow. In Table 2B, it is shown that no effect on propylene activity was found upon the addition of ~8 Ca^{2+} cations per unit cell, thus excluding trace divalent cations as the major source of propylene formation. The results shown in Table 2B could be rationalized by the fact that the 550°C calcination may have caused dehydroxylation with irreversible migration of the Ca^{2+} cations into the sodalite cages (26). Another source for propylene formation on the fully exchanged, unrinsed samples could be from a propoxide intermediate and appears to be a likely candidate at this time (Chapter 2).

Intrinsic rates of acetone formation over the unrinsed hydroxide exchanged X and Y zeolites are listed also in Table 2A. A large increase in acetone formation was found

Table 2. Intrinsic Reaction Data from Isopropnanol Decomposition.

	Catalyst		Calcination Atmosphere	Acetone Rate[e]	Propylene Rate[e]	% Acetone Selectivity[f]
A)	Na	X[b]	He	70	2003	3.38
	KNa	X[b]	He	295	88	77.0
	RbNa	X[b]	He	264	106	71.4
	CsNa	X[b]	He	120	102	54.1
	Na	Y[b]	He	144	40	78.3
	KNa	Y[b]	He	1158	51	95.8
	CsNa	Y[b]	He	1052	51	95.4
B)	CaCsNa	Y[b,c]	He	1025	43	96.0
	CsNa	Y[b]	He	1052	51	95.4
C)	Cs-Ace/$Cs_{39}Na_{19}$	Y[d]	He	3497	94	97.4
	Cs-Ace/$Cs_{25}Na_{33}$	Y[d]	He	2555	79	97.0
	Cs-Ace/$Cs_{56}Na_{26}$	X[d]	He	527	328	61.6
D)	Cs-Ace/CsNa	Y[d]	O_2	4313	118	97.3
	Cs-Ace/CsNa	Y[d]	He	3497	94	97.4

a) Start-up procedure 1.

b) Exchanged via hydroxide and unrinsed.

c) ~8 Ca^{2+} per unit cell

d) ~2.0 Cesium acetate molecules per unit cell

e) mol • (mol of zeolite unit cells)$^{-1}$ • hr^{-1}

f) % Acetone Selectivity = acetone yield/ (acetone yield + propylene yield) X 100%

when Na^+ was exchanged by K^+ for both zeolite X and Y. For zeolite X, the acetone activity and selectivity were found to be the highest for KNaX. It was the Y zeolite, however, which showed the best acetone activity and selectivity. This enhanced activity of the Y zeolite over the X zeolite was not expected on the basis of data in a prior investigation (17) which suggested X zeolite to be more basic. However, the influence of excess alkali must be taken into consideration (*vide infra*).

Because of its high activity and selectivity for acetone formation, zeolite Y exchanged with Cs^+ was chosen to investigate further the factors which may influence base activity.

2.4.4 Influence of the Calcination Temperature

Figure 2 illustrates the yields of acetone and propylene at 350°C as a function of calcination temperature for CsNaY-OH-UR. A small decrease in both the yields of acetone and propylene was observed when the calcination temperature was above 500°C. However, little variation in selectivity was obtained when the catalyst was calcined between 450°C and 600°C. The loss in crystallinity from calcination ranged from 4% at 450°C to 11% at 600°C (measured by adsorption).

Interestingly, the rate at which the calcination temperature was achieved played a critical role in the stability of the acetone and propylene activity. Figure 3 shows the effect of the heating rate to reach the calcination temperature on the acetone and propylene activity. These activities were determined using start-up procedure 2 with CsNaY-OH-UR. Two heating rates were employed; 2 and 20 °C/min. For both heating rates, the initial acetone and propylene activities were similar. However, for the heating rate of 2°C/min, the acetone activity quickly fell to zero while the propylene activity rose sharply. Attempts to re-establish initial activity by reactivating the catalyst in helium

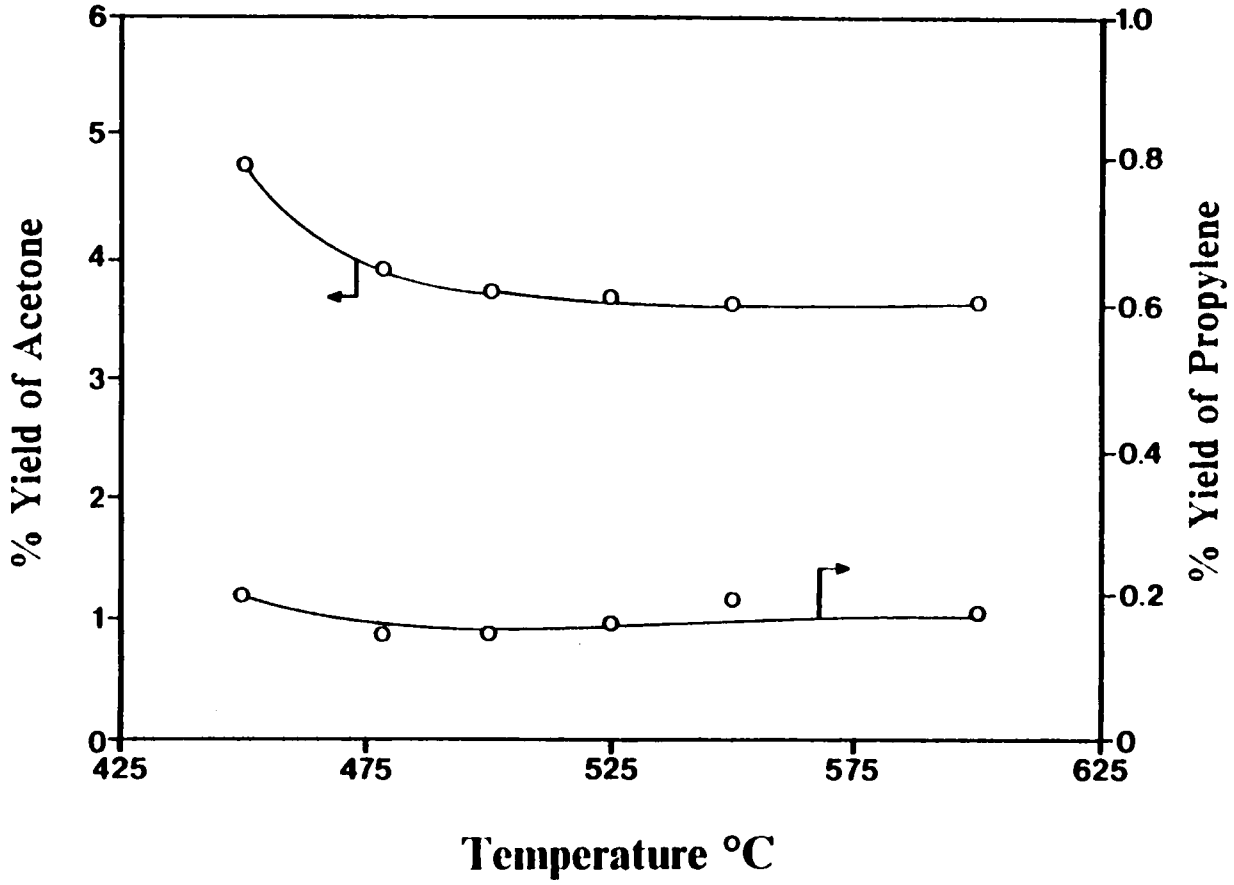

Figure 2 Influence of Calcination Temperature on Activity. Calcination atmosphere was helium and the heating rate was 20°C/min. F/W = 1.44 mol isopropanol •hr $^{-1}$ • g $^{-1}$, temperature = 350°C, total pressure = 1 atm., and partial pressure of isopropanol = 152 torr(STP). Start-up procedure 1.

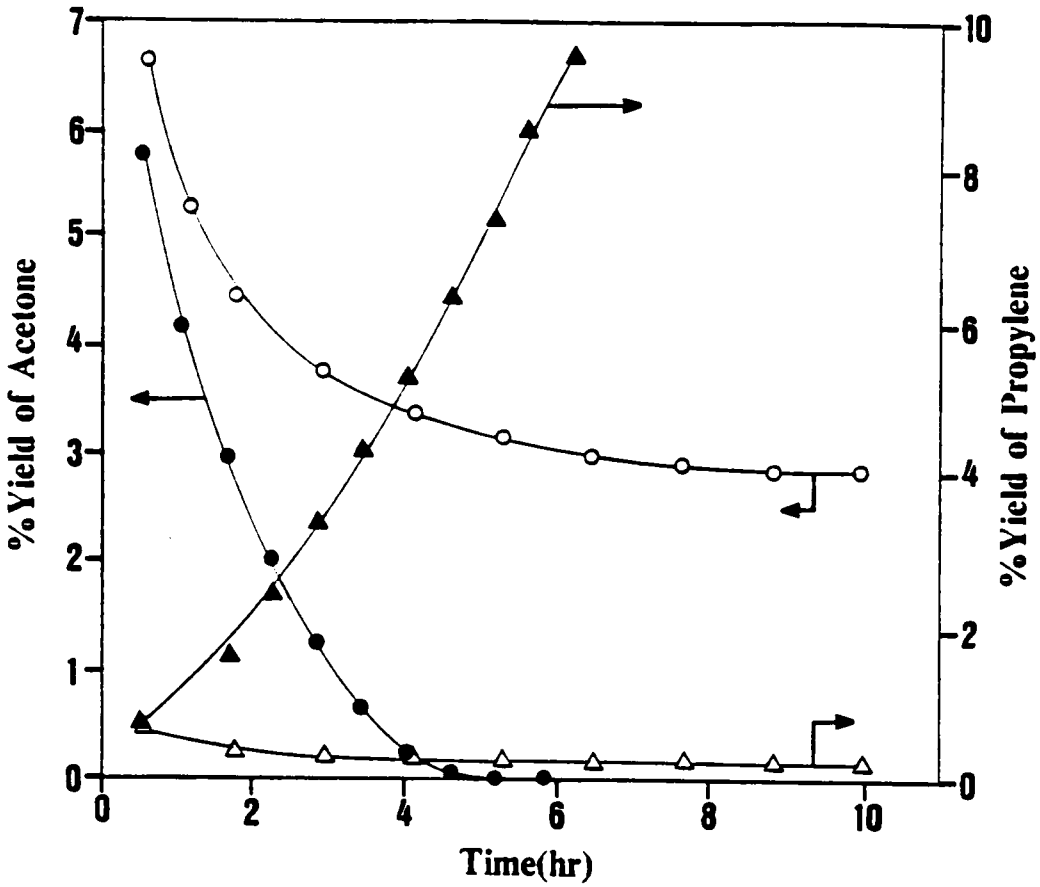

Figure 3 **Influence of Heating Rate on Activity.** 2° C/min: ● , acetone; ▲ , propylene and 20°C/min: ○ , acetone; △ , propylene. F/W = 0.90 mol isopropanol • hr^{-1} • g^{-1}, temperature = 350°C, total pressure = 1 atm., and partial pressure of isopropanol = 152 torr. Start-up procedure 2.

lium or air failed. For the heating rate of 20°C/min, both the acetone and propylene activity achieved a steady state value. Little is understood at this point why the heating rate affects the activity, but it does appear from Figure 3 that propylene activity is growing at the expense of acetone activity for the heating rate of 2°C/min.

2.4.5 Influence of the Exchange Salt

Zeolite Y was exchanged with cesium hydroxide, acetate, nitrate and chloride to investigate the influence of the exchange salt on activity. Figure 4A shows the effect of the exchange salt on acetone activity of the rinsed catalysts. The hydroxide, acetate, and nitrate exchanged zeolites had approximately the same level of acetone activity with little variation between the initial and steady state activity. The chloride exchanged zeolite showed a lower level of acetone activity which may be a result of occluded chloride reducing the electron donating potential of the system. The propylene activity of the rinsed catalysts is shown in Figure 4B. Approximately the same level of propylene activity was found for the hydroxide, acetate, and nitrate exchanged zeolites. For the chloride exchanged zeolite, however, a significant increase in propylene activity was observed.

Figure 5 shows the acetone activity of the unrinsed hydroxide, acetate, nitrate, and chloride exchanged zeolites. For the unrinsed hydroxide and acetate exchanged zeolites, the initial acetone activity was increased by a factor of five above the rinsed analogs. This acetone activity slowly declined but remained higher than the activity recorded from the rinsed materials. For the unrinsed nitrate exchanged zeolite, the acetone activity increased by a factor of 2 but ultimately reached the activity recorded from its rinsed

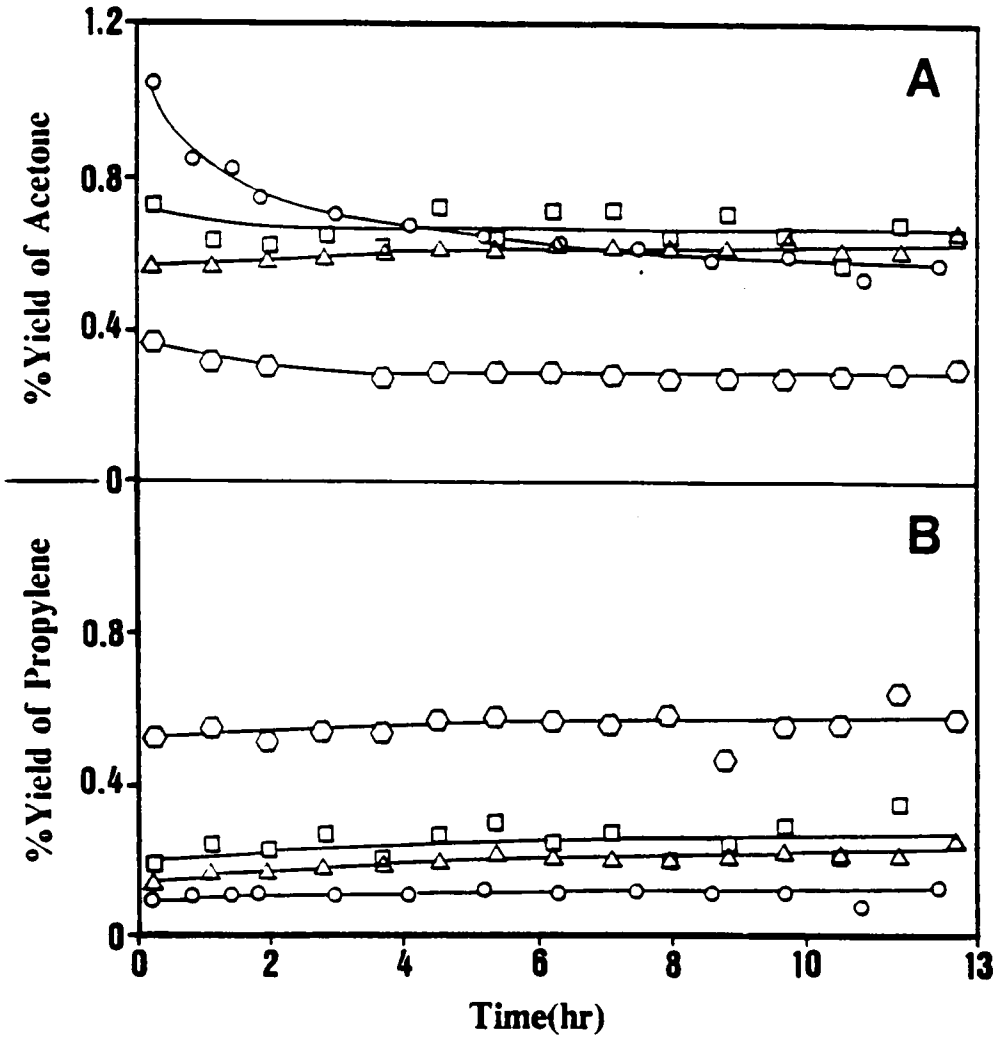

Figure 4 **Influence of Exchange Salt on: (A), Acetone; and (B), Propylene Activity of Rinsed Zeolites.** ○ , hydroxide; □ , acetate; △ , nitrate; ⬡ , chloride. F/W = 2.41 mol isopropanol • hr^{-1} • g^{-1}, temperature = 350°C, total pressure = 1 atm., and partial pressure of isopropanol = 152 torr(STP). Start-up procedure 2.

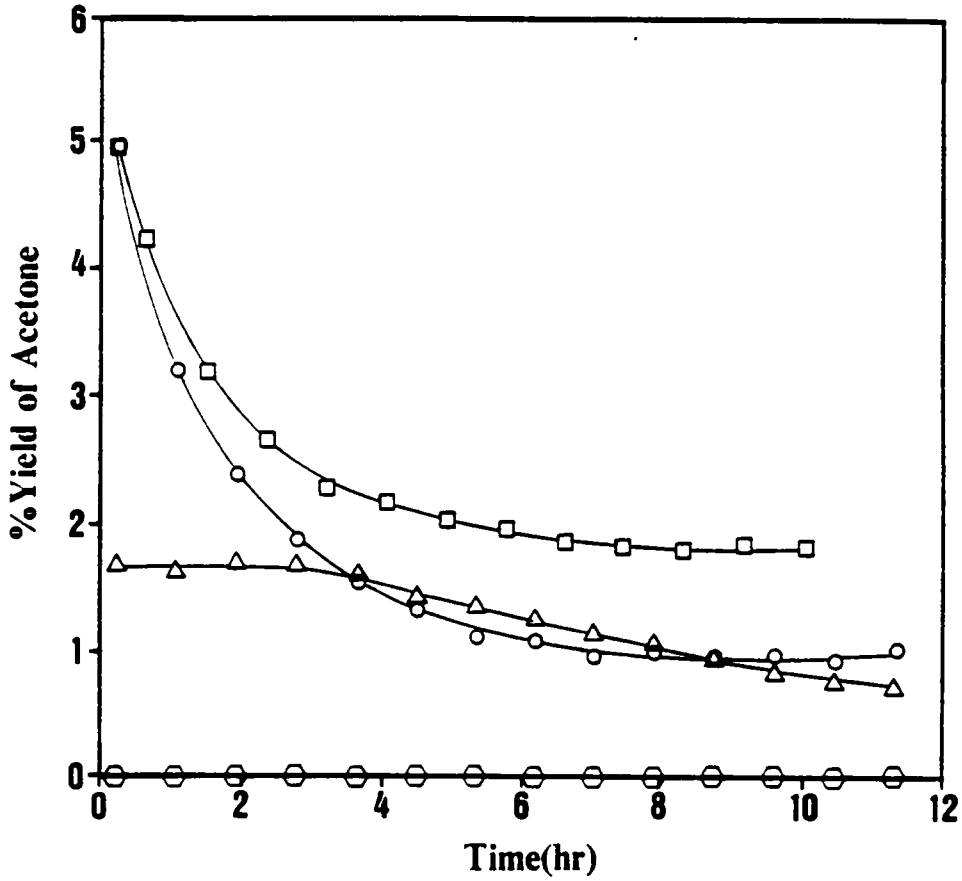

Figure 5 **Influence of Exchange Salt on Acetone Activity of Unrinsed Zeolites.** ○ , hydroxide; □ , acetate; △ , nitrate; ⬡ , chloride. F/W = 2.41 mol isopropanol • hr^{-1} • g^{-1}, temperature = 350°C, total pressure = 1 atm., and partial pressure of isopropanol = 152 torr. Start-up procedure 2.

analog. Interestingly, for the unrinsed, chloride exchanged zeolite, complete elimination of acetone activity was observed.

The propylene activity (not shown) of the unrinsed hydroxide, acetate, and nitrate exchanged zeolites fell below the activities recorded from the rinsed materials by ~40% suggesting that the higher propylene activity of the rinsed catalysts may be a result of decationation during the rinsing step (22). Propylene activity for the unrinsed chloride exchanged zeolite was identical to that of its rinsed analog.

From the results provided thus far, there exist considerable differences in activity between the rinsed and unrinsed hydroxide and acetate exchanged Y zeolites. Two possible explanations could be offered for these differences. One is that by rinsing the zeolite after filtration, decationation of the zeolite occurs to some degree (22), thus lowering the acetone activity and increasing the propylene activity. The other possible explanation is that by leaving the zeolite unrinsed, occluded hydroxide or acetate remains which upon calcination provides a second more active base site. To answer these questions, it was first establish that by leaving the zeolite unrinsed alkali salt is occluded. Since the acetate ion (CH_3CHOO^-) is observable by infrared spectroscopy and combustible in air, the unrinsed, acetate exchanged Y zeolite (CsNaY-Ace-UR) was examined for occluded cesium acetate by infrared spectroscopy and differential thermal analysis (DTA).

Figure 6 shows the DTA patterns for the rinsed and unrinsed acetate exchanged zeolite. For both cases, the loss of water is reflected by a broad endotherm located between 25°C and 350°C. Unlike the rinsed zeolite a sharp exotherm occurs for the unrinsed zeolite at 450°C. Peaks in this region are attributed to the exothermic oxidation of carbon (this peak is absent when the DTA was performed in a helium atmosphere, yet we know the active site is formed in either helium or oxygen (*vide infra*)).

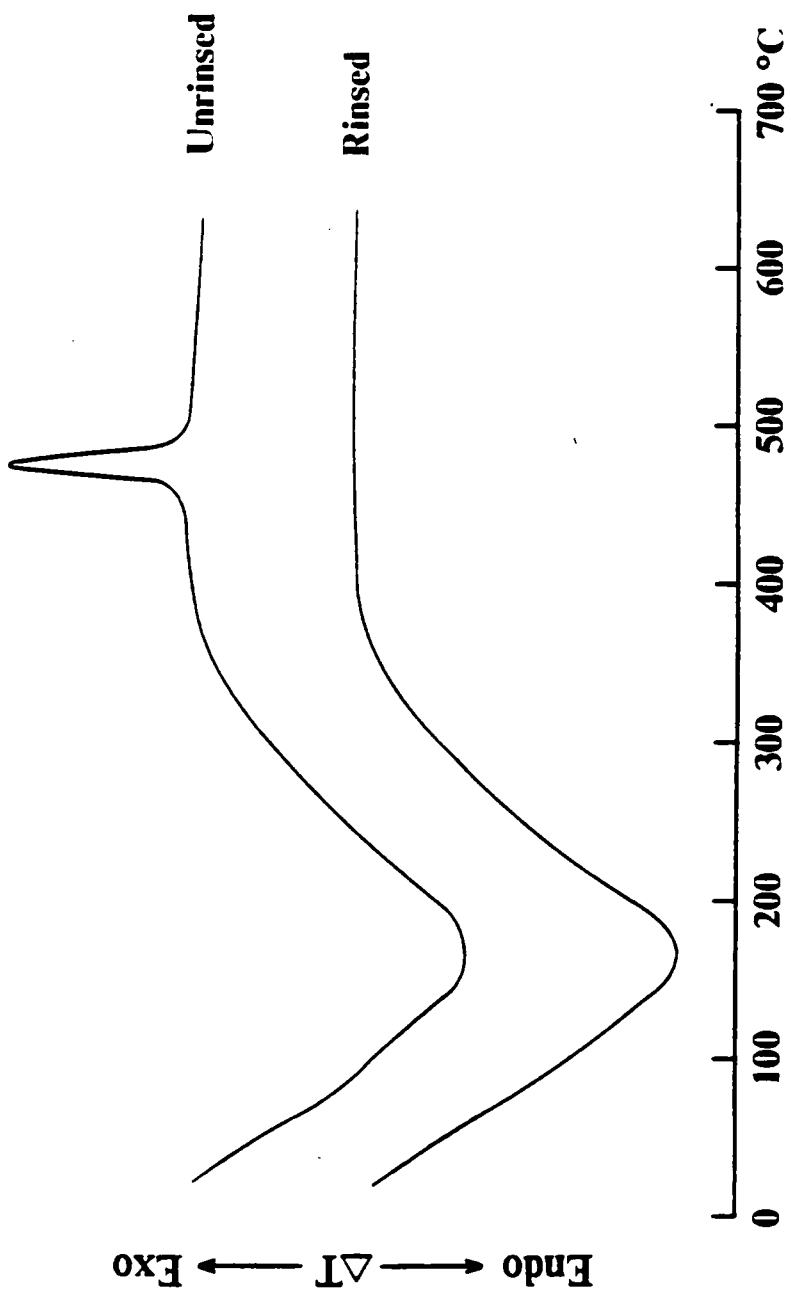

Figure 6 Differential Thermal Analysis of Unrinsed and Rinsed Cesium Acetate Exchanged Y Zeolite.

To further investigate the presence of excess cesium acetate, the unrinsed zeolite was examined by FTIR. Figure 7A shows the IR spectrum for cesium acetate pressed in KBr. Kakihana et al. (31) investigated sodium acetate by infrared spectroscopy. Based upon their results we have assigned the the vibrational frequencies observed for cesium acetate. The broad absorption at 3307 cm^{-1} is in the OH region and is most likely due to trace water. Although not very pronounced, the band observed at 2985 cm^{-1} is assigned to the asymmetric CH_3 stretch. This general weakness, however, is consistent with a CH_3 group adjacent to a carbonyl-derived group such as COO^- (4). The band at 1570 cm^{-1} is assigned to the asymmetric CO stretch. For sodium acetate, several frequencies were assigned in the 1440 - 1420 cm^{-1} region. The main contribution, however, occurs from the asymmetric CH_3 deformation and the symmetric CO stretch. Therefore, the band observed at 1399 cm^{-1} in the cesium acetate spectrum is most likely due to one or more of those vibrations. The small shoulder at 1334 cm^{-1} is identical to the value reported by Kakihana et al. (31) for the symmetric CH_3 deformation.

For the unrinsed zeolite, a spectrum was recorded at 250, 350, and 450°C in air. The asymmetric and symmetric C-H bands at 2955 and 2911 cm^{-1} are very strong at 250°C clearly indicating the presence of occluded acetate. These bands appear also at 350°C, but disappear after ~30 minutes (Fig. 7D). At 450°C several bands are still present. The band at 3732 cm^{-1} is assigned to the terminating silanol group and is in good agreement with the value of 3740 cm^{-1} reported by Ward (32) for CsNaY. Small broad bands are observed also at 450°C between 1710 and 1366 cm^{-1} which are in the region for carbonate absorption. The band at 2143 cm^{-1} is not assigned as yet.

The absorptions for the acetate ion at 1570 and 1399 cm^{-1} (Fig. 7A) appear to align with the bands at 1578 and 1378 cm^{-1} for the unrinsed zeolite (Fig 7B). However, the band at 1578 cm^{-1} is assigned as overlapping CO stretching bands for the occluded acetate ion and also a carbonate species. Furthermore, the band at 1378 cm^{-1} appears

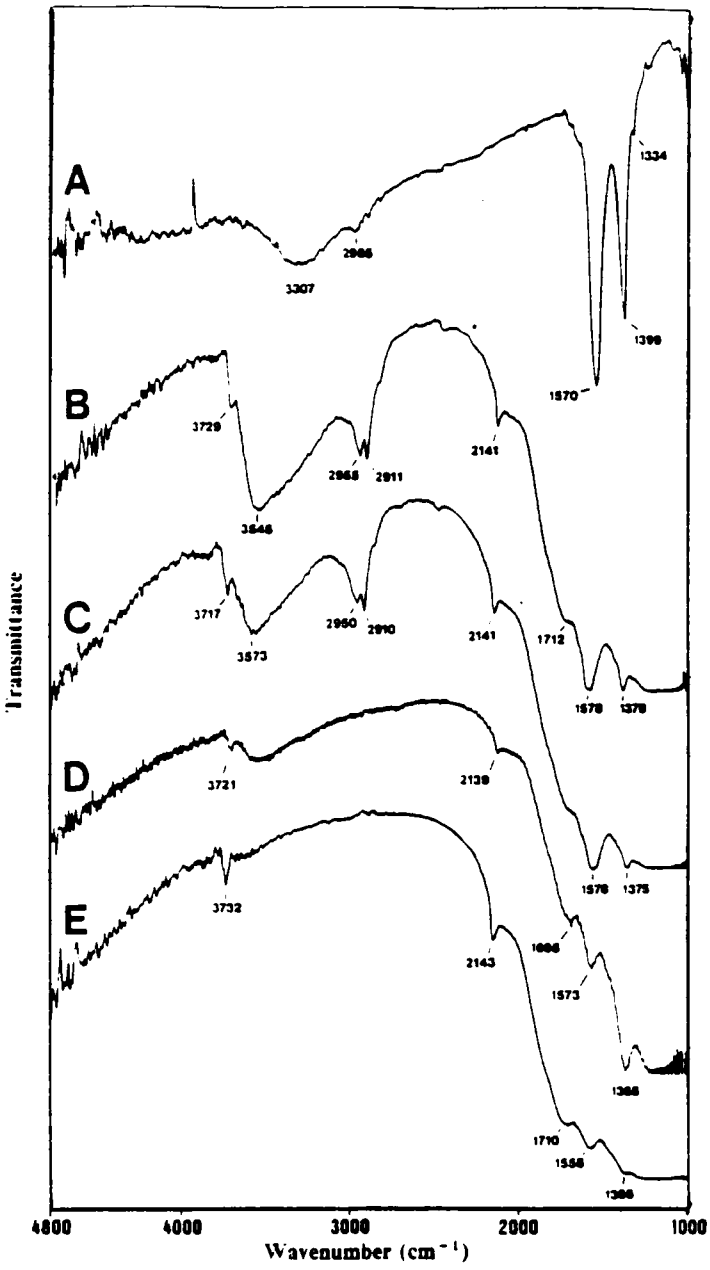

Figure 7 **FTIR Spectra of Cesium Acetate and CsNaY-Ace-UR:** (A), cesium acetate in KBr at 25°C; the unrinsed cesium acetate exchanged Y zeolite at (B), 250°C; (C), 350°C for 5 mins; (D), 350°C for 30 mins; and (E), 450°C in air.

to be strictly from a carbonate species. These assignments are supported by the FTIR studies of CsNaY-OH-UR (Figs. 8B and 8C) which contains no acetate ions but has similar base properties to CsNaY-Ace-UR (*vide supra*). Figures 8B and 8C show the IR spectra of CsNaY-OH-UR in air at 150 and 350°C, respectively. The doublet at 1381 and 1317 cm^{-1} (Fig. 8B) along with the band at 1580 cm^{-1}(Fig. 8C) which appears after removal of water (1647 cm^{-1}) are in fair agreement with Bertsch and Habgood (33) who observed from CO_2 adsorption on KNaX bands at 1570, 1380, and 1340 cm^{-1}. CsNaY-Ace-UR at 150°C (Fig. 8A) shows a similar doublet at 1387 and 1329 cm^{-1}. However, a strong absorption at 1578 cm^{-1} along with a shoulder at 1427 cm^{-1} appears also. The band at 1578 cm^{-1} is postulated to be the asymmetric CO stretch of the occluded acetate ion. The shoulder observed at 1427 cm^{-1} which is in the region of 1440-1420cm^{-1} reported by Kakihana et al. (31) for sodium acetate is postulate to be resulting from the occluded acetate as well. Note that after the CH stretch has disappeared at 350°C (Fig. 7D) (suggesting the decomposition of the acetate) the bands at 1573 and 1368 cm^{-1} are still present. Bands in this region are observed also for the CsNaY-OH-UR at 350°C at 1580 and 1366 cm^{-1} supporting further their assignment to carbonate species.

Carbonate absorptions at 1580 and 1381 cm^{-1} are observed momentarily for the rinsed, acetate exchanged Y zeolite at 150°C (not shown). However, they disappear upon longer heating. The higher thermal stability of the carbonates on the unrinsed, hydroxide and acetate exchanged CsNaY zeolites agrees with the results of King and Garces (34) who observed that the temperature required to eliminate carbonates from the less basic LiX and NaX zeolites occurred at approximately 400°C. However, they detected considerable amounts of carbonate on the KNaX, RbNaX, and CsNaX at 450°C. King and Garces suggested that this increase in the thermal stability of the

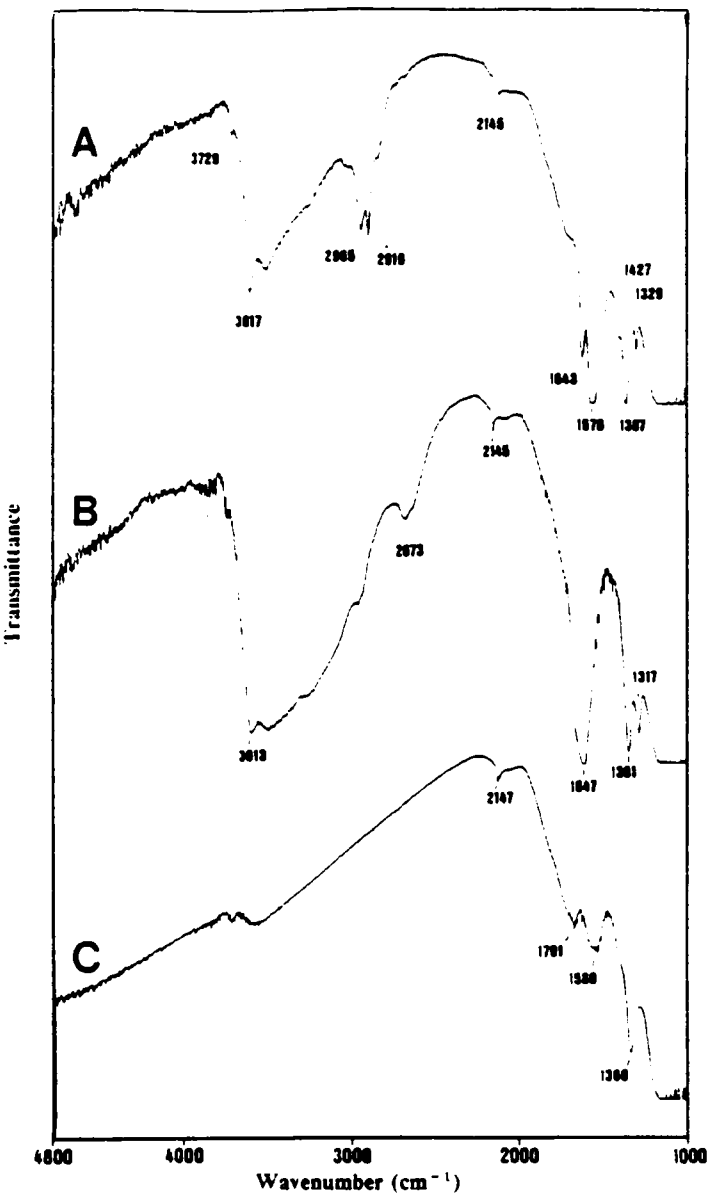

Figure 8 FTIR Spectra of CsNaY-OH-UR and CsNaY-Ace-UR: (A), CsNaY-Ace-UR at 150°C; (B), CsNaY-OH-UR at 150°C; and (C), CsNaY-OH-UR at 350°C in air.

carbonates is a result of the higher base strength associated with the K^+, Rb^+, and Cs^+ exchanged X zeolites.

From DTA and FTIR spectroscopy, cesium acetate was detected on the unrinsed zeolite while it was not for the rinsed zeolite. Also, the reaction rate data clearly show a significant increase in acetone activity for the unrinsed, acetate exchanged zeolite. It, therefore, appears that the differences in activity between the rinsed and unrinsed, hydroxide and acetate exchanged zeolites are not due to a loss in activity from decationation but rather a gain in activity associated with the occluded exchange salt. If this is the case, a second type of base site formed by the decomposition of the occluded cesium salt may be present.

2.4.6 Influence of Cesium Loading

Cesium was exchanged into NaY at loadings of ~ 1 Cs^+ per unit cell to a full exchange of 39 Cs^+ per unit cell (maximum exchange obtained here with a 0.1N solution). The fully exchanged and all partially exchanged zeolites were rinsed with deionized water to remove any residual exchange salt. Cesium loadings above 100% ion exchange were achieved by occluding via exposure to exchange solutions of 0.3-0.5N between 3 and 5 cesium acetate molecules per unit cell into the fully exchanged Y zeolite. Figure 9 illustrates the effect of cesium loading on both acetone and propylene activity. The catalysts with lower levels of cesium showed no detectable acetone formation but very high rates of propylene formation. The high propylene activity was most likely the result of decationation from the rinsing, for very little propylene activity was recorded from the unrinsed NaOH exchanged Y zeolite (Table 2A). However, as more Cs^+ was exchanged into the zeolite the propylene rate declined while the acetone rate rose. Only after 100%

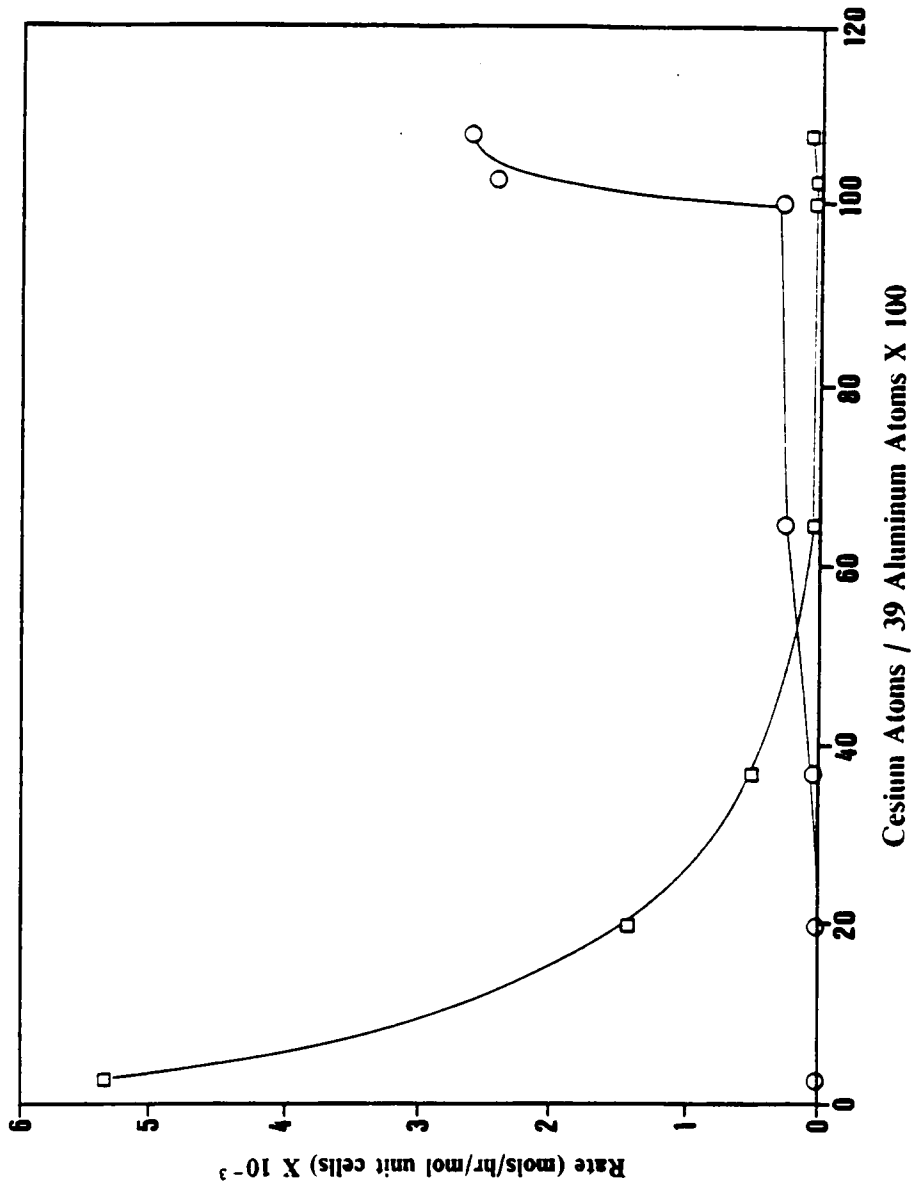

Figure 9 **Influence of Cesium Loading on Activity of Y Zeolite.** ○, acetone; □, propylene. Temperature = 350°C, total pressure = 1 atm., and partial pressure of isopropanol = 152 torr(STP). Start-up procedure 1.

ion exchange was exceeded and between 3 and 5 excess cesium acetate molecules per unit cell were occluded into the zeolite does an abrupt rise in the acetone activity occur. It is this abrupt rise that strongly suggests the presence of a second very active base site which appears to be from the decomposition products of the cesium acetate. Acetone activity associated with the rinsed CsNaY could, therefore, result from the lattice oxygens as suggested by other authors (14,17).

2.4.7 Influence of CO_2 Contact

Because of the electrophilic nature of CO_2, adsorption onto active base sites, e.g., O^{2-}, can occur and subsequently block base catalyzed activity (35). Furthermore, the nature of the base site can affect the adsorption of CO_2 (35) as well as the thermal stability of the adsorbed species. One might, therefore, expect different catalytic behavior during and perhaps after CO_2 contact (36). Both the rinsed and unrinsed Y zeolite exchanged with cesium hydroxide, acetate, nitrate, and chloride were contacted with CO_2 during reaction conditions. After steady state was achieved, CO_2 was introduced into the reactant feed at 5 torr for 2 hours (helium was decreased to maintain a constant partial pressure of isopropanol).

For rinsed zeolites (Fig. 10), acetone activity was suppressed in the presence of CO_2. Upon removal of CO_2 from the feed which contacted the acetate, nitrate, and chloride exchanged zeolites, acetone activity returned immediately to the steady state value. Upon CO_2 removal from the feed which contacted the rinsed hydroxide exchanged zeolite, a small increase in acetone activity was observed which may suggest incomplete rinsing of the zeolite (*vide infra*).

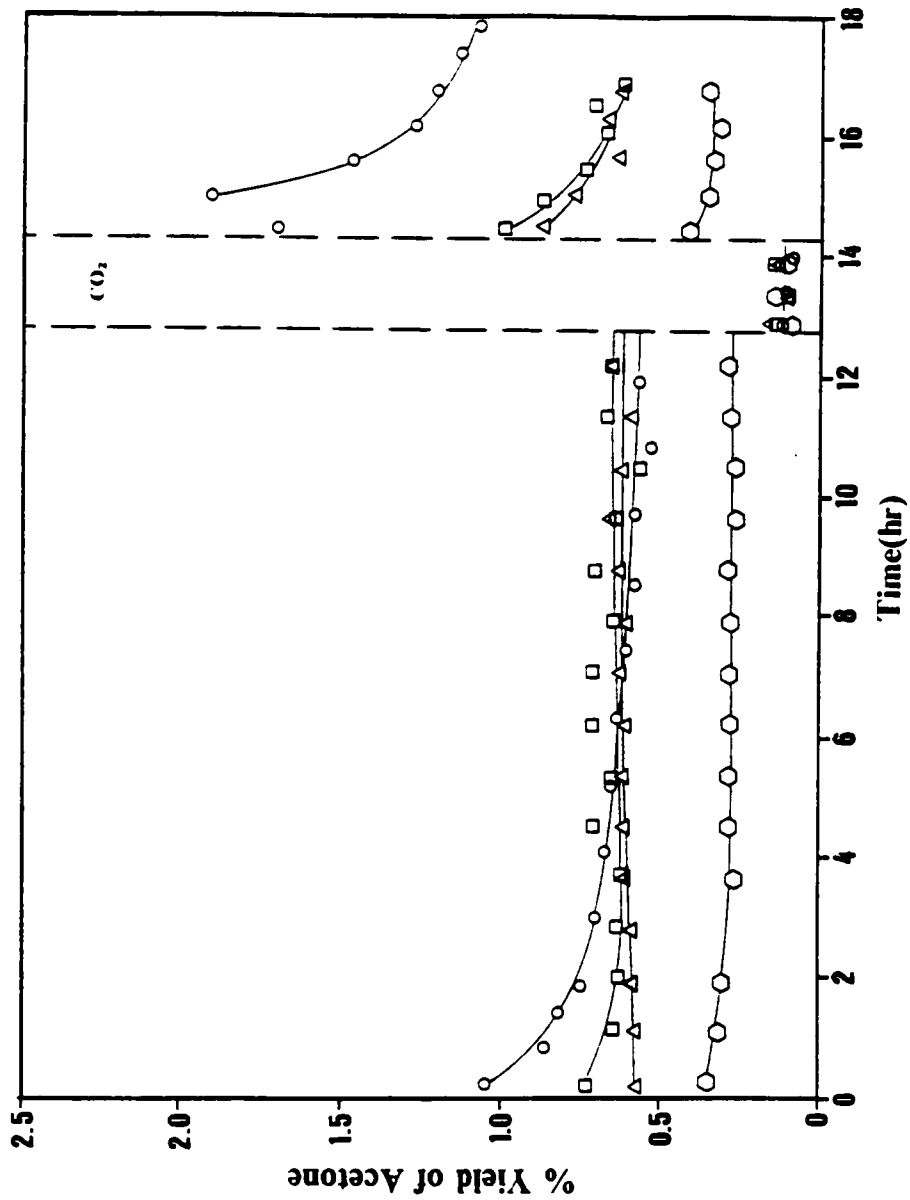

Figure 10 Influence of CO_2 Contact on Activity of Rinsed Y Zeolites. ○, hydroxide; □, acetate; △, nitrate; ⬡, chloride. F/W = 2.41 mol isopropanol • hr^{-1} • g^{-1}, temperature = 350°C, total pressure = 1 atm., and partial pressure of isopropanol = 152 torr(STP). Start-up procedure 2.

Figure 11 shows the influence of CO_2 on the acetone activity of the unrinsed zeolites. The acetone activity of the unrinsed hydroxide and acetate exchanged zeolites was very high initially, but declined slowly to lower levels of activity. Contact of CO_2 with these catalysts suppressed acetone activity. Upon removal of CO_2 from the feed, the high activity observed at initial times was re-establish which may suggest that some base sites were being reactivated by CO_2 contact. Further evidence to suggest that some base sites could be reactivated by CO_2 contact and removal is given by the activity data from the unrinsed, nitrate exchanged zeolite. As shown in Figure 11, the initial and steady state acetone activity of the unrinsed nitrate exchanged zeolite are fairly similar. However, after CO_2 contact, the acetone activity was promoted to the high levels observed for the unrinsed hydroxide and acetate exchanged zeolites.

2.4.8 Influence of Support

To investigate the role of the CsNaY zeolite in the formation of the base site via cesium acetate decomposition, cesium acetate was impregnated at ~2.4wt% on CsNaY, silica gel, and activated carbon. Figures 12B and 12D show the DTA patterns for the decomposition of cesium acetate on CsNaY and the silica gel, respectively. For the silica support, a broad exotherm is shown at 300°C. However, for CsNaY a sharp exotherm occurs at ~475°C suggesting the decomposition mechanism differs for the two supports. Also, cesium acetate supported on silica gel and activated carbon showed no acetone formation at 350°C, and only trace propylene activity was observed for the silica support. From the reaction rate data and DTA patterns, it appears that CsNaY does play an active role in the decomposition of cesium acetate to an active base site.

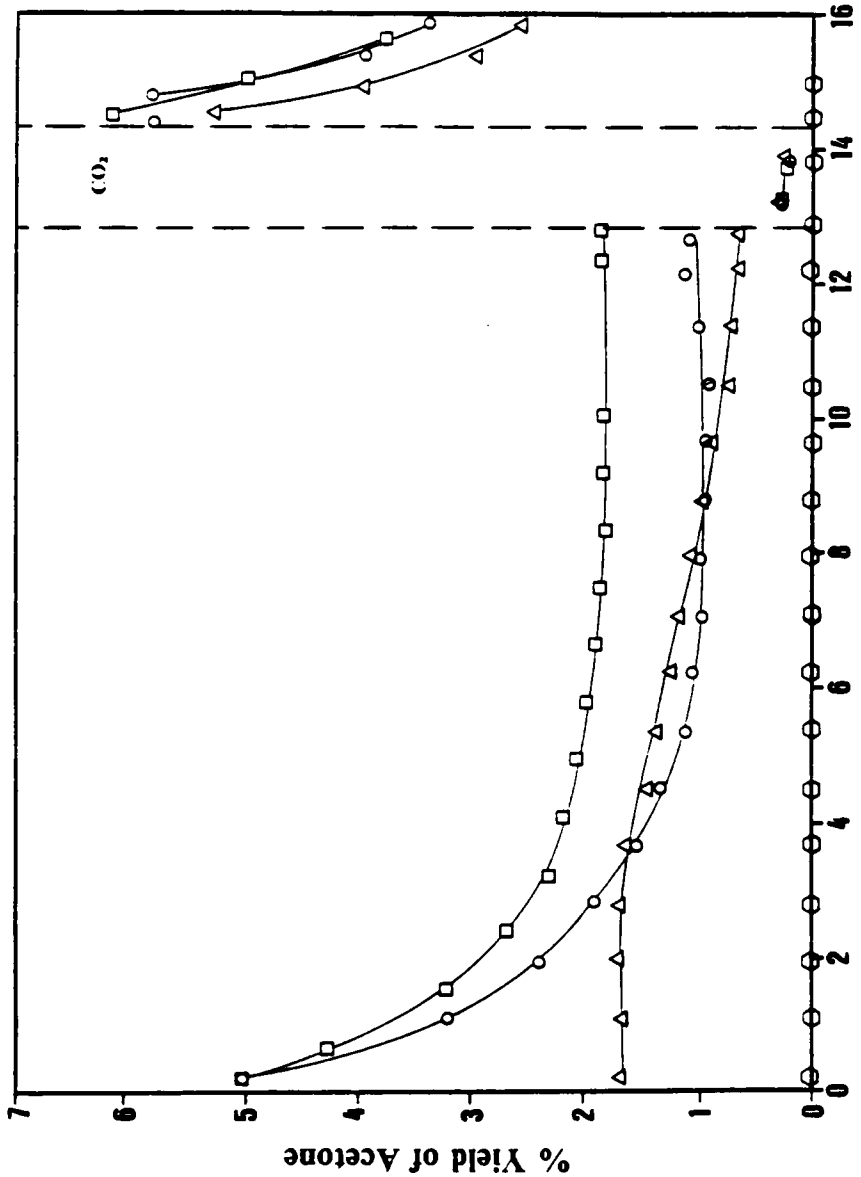

Figure 11 Influence of CO_2 Contact on the Activity of Unrinsed Y Zeolites. ○, hydroxide; □, acetate; △, nitrate; ⬡, chloride. $F/W = 2.41$ mol isopropanol • hr^{-1} • g^{-1}, temperature = 350°C, total pressure = 1 atm., and partial pressure of isopropanol = 152 torr(STP). Start-up procedure 2.

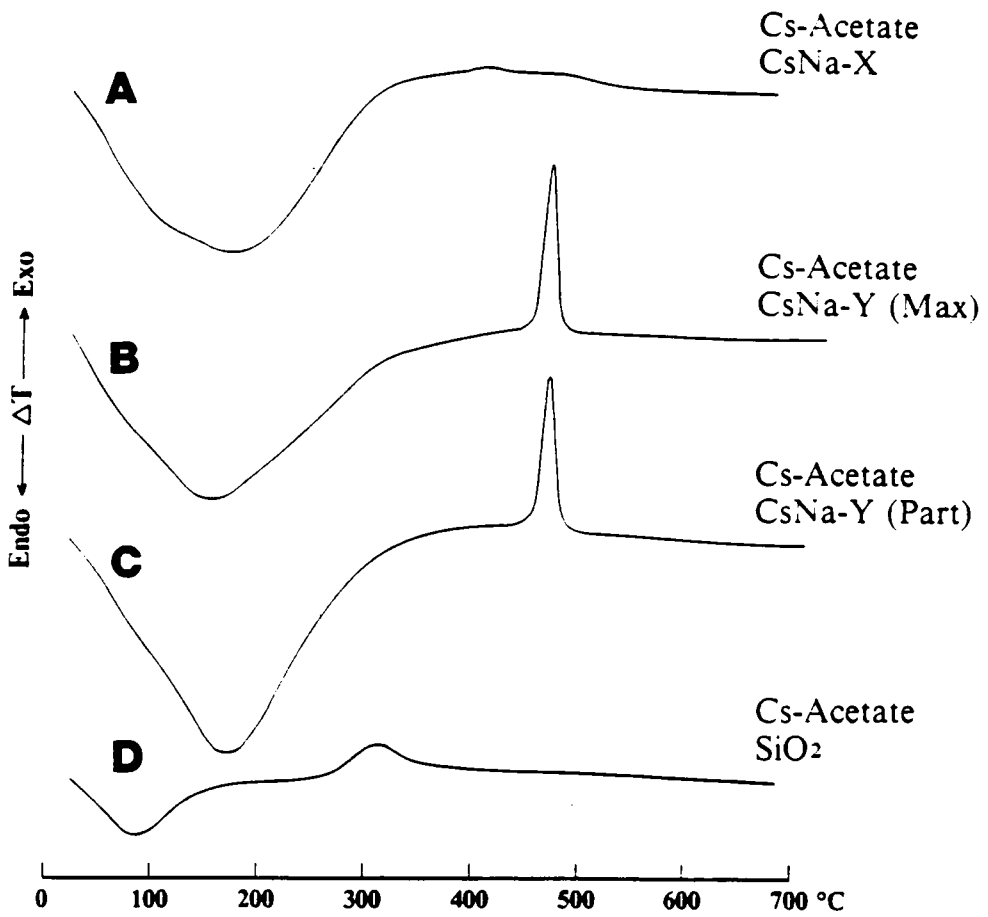

Figure 12 Differential Thermal Analysis: (A), 2.0Cs-ace/$Cs_{56}Na_{26}X$; (B), 2.0Cs-ace/$Cs_{39}Na_{19}Y$; (C), 2.0Cs-ace/$Cs_{25}Na_{33}Y$; (D), 2.4wt% Cs-acetate/SiO_2.

It was shown previously that CsNaX-OH-UR was less effective for acetone formation than CsNaY-OH-UR (Table 2A). To investigate this further, cesium acetate was impregnated at approximately 2.0 cesium acetate molecules per unit cell into (i) a $Cs_{56}Na_{26}X$ zeolite , (ii) a fully exchanged $Cs_{39}Na_{19}Y$ zeolite ,and (iii) a partially exchanged $Cs_{25}Na_{33}Y$ zeolite. Infrared studies confirm the presence of occluded cesium acetate for these three catalysts. Because zeolite X is difficult to exchange fully, the partially exchanged Y zeolite (iii) was used also to investigate the possibility that during impregnation of X zeolite, Na^+ ions were being exchanged by cesium acetate to form sodium acetate. Table 2C gives the rate of acetone and propylene formation per unit cell for the three catalysts. The partially exchanged Y zeolite showed high acetone activity and selectivity. Therefore, we exclude the possibility that all the cesium acetate exchanges with Na^+ ions during impregnation. Low acetone activity and selectivity were found for the X zeolite. To determine whether the decomposition mechanism of the acetate is similar for the X and Y zeolite, differential thermal analysis was performed in air. From Figure 12, the fully and partially exchanged Y zeolites have the sharp exotherm at 475°C suggesting that the decomposition of the acetate occurs in an identical fashion on these materials. However, this decomposition process does not appear to occur for the X zeolite as evidenced by the small broad exotherm located between 350 and 500°C.

2.4.9 Influence of Calcination Atmosphere

CsNaY impregnated with ~2.4wt% cesium acetate was calcined with helium (99.995$^+$%) and oxygen (99.5$^+$%) to investigate how these gases influence the decomposition of the acetate to an active base site. The results are given in Table 2D. With

the oxygen calcination, both the acetone and propylene activity were slightly greater than that obtained from the helium atmosphere. Interestingly, the calcination atmosphere had no effect on selectivity. This might suggest that the decomposition products are similar in both calcination atmospheres, however, the oxygen calcination appears to be slightly more effective for the production of active sites

2.4.10 Comparison to MgO

MgO formed by the dehydroxylation of $Mg(OH)_2$ was used so that a comparison could be made between our zeolite activities here and those reported in the open literature for other metal oxides. From data given by Tanabe (38), it was shown that to achieve the optimal number of base sites in the transformation of $Mg(OH)_2$ to MgO, the calcination temperature should be between 550°C and 600°C. Therefore, $Mg(OH)_2$ was heated in helium to 550°C for 4 hours. Start-up procedure 1 was used to determine the reaction rates. Table 3 shows that on a surface area basis, the acetone activity for CsNaY zeolite modified with ~2.4wt% cesium acetate is slightly greater than that observed for the MgO catalyst at 350°C.

2.5 Conclusions

It is concluded from this work that upon calcination, a very active base site is formed by the decomposition of cesium acetate supported on CsNaY zeolite. Upon impregnation of CsNaX and CsNaY with identical loadings of cesium acetate, the

Table 3. Activity Comparison Between MgO and Acetate Impregnated CsNaY

Catalyst	BET Area (m^2 g)[c]	Acetone Rate (mol/hr/m^2 X 10^6)	Propylene Rate (mol/hr/m^2 X 10^6)	% Acetone Selectivity[d]
MgO[a]	125	334	7.9	97.7
Cs-Ace/CsNaY[b]	492	406	10.9	97.4

a) Derived from $Mg(OH)_2$

b) ~2.0 cesium acetate molecules per unit cell.

c) BET surface areas calculated from O_2 adsorption data.

d) % Acetone Selectivity = acetone yield/ (acetone yield + propylene yield) X 100%

acetone activity of the impregnated CsNaY zeolite is an order of magnitude greater than that found for the impregnated CsNaX zeolite. The impregnated CsNaY is found also to show an order of magnitude greater acetone activity than the parent CsNaY zeolite. Furthermore, for the impregnated CsNaY zeolite, the selectivity to acetone is above 97%, and on a surface area basis, the acetone activity is slightly greater than that found for MgO.

2.6 *References*

1. Barthomeuf, D., Coudurier, G., and Vedrine, J. C., Mater. Chem. Phys. **18**, 553 (1988).
2. Krylov, O. V., "Catalysis by Non-Metals." p. 118. Academic Press, New York, 1970.
3. Gentry, S. J., and Rudham, R., J. Chem. Soc. Faraday Trans. I **70**, 1685 (1974).
4. Zaki, M. I., and Sheppard, N., J. Catal. **80**, 114 (1983), and references therein.
5. Miyata, H., Wakamiya, M., and Kubokawa, Y., J. Catal. **34**, 117 (1974).
6. Koga, O., Onishi, T., and Tamaru, K., J. Chem. Soc. Faraday Trans. I **76**, 19 (1980).
7. Kim, K. S., Barteau, M. A., and Farneth, W. E., Langmuir **4**, 533 (1988).
8. Parrott, S. L., Rodgers, Jr., J. W., and White, J. M., Appl. Surf. Sci. **1**, 443 (1978).
9. Bowker, M., Petts, R. W., and Waugh, K. C., J. Chem. Soc. Faraday Trans. I **81**, 3073 (1985).
10. Waugh, K. C., Bowker, M., Petts, R. W., Vandervell, H. D., and O'Malley, J., Appl. Catal. **25**, 121 (1986).
11. Bowker, M., Petts, R. W., and Waugh, K. C., J. Catal. **99**, 53 (1986).
12. Noller, H. and Ritter, G., J. Chem. Soc. Faraday Trans. I **80**, 275 (1984).
13. Cunningham, J., Hodnett, B. K., Ilyas, M., Tobin, J., and Leahy, E. L., Discuss. Faraday Soc. **72**, 283 (1981).
14. Yashima, T., Suzuki, H., and Hara, N., J. Catal. **33**, 486 (1974).
15. Nagy, J. B., Lange, J. -P., Gourge, A., Bodart, P., and Gabelica, Z., in "Catalysis by Acids and Bases"(B. Imelik et al., Eds.), Vol. 20, p. 127. Elsevier, Amsterdam, 1980.
16. Derewinski, M., Haber, J., and Ptaszynski, J., in "New Developments in Zeolite Science and Technology"(Ymorakam et al. Eds.), p. 57. Elsevier, Amsterdam, 1986.
17. Barthomeuf, D., J. Phys. Chem. **88**, 42 (1984).
18. Unland, M. L., and Baker, G. E., in"Catalysis of Organic Reactions" (W.R. Moser, Ed.), p. 51. Dekker, New York, 1981.
19. Garces, J. M., Vrieland, G. E. Bates, S. I., and Scheidt, F. M., in "Catalysis by Acids and Bases"(B. Imelik et al., Eds.), Vol. 20, p. 67. Elsevier, Amsterdam, 1985.
20. Engelhardt, J., Szanyi, J. and Valyon, J., J. Catal. **107**, 296 (1987).

21. Martens, L. R., Vermeiren, W. J., Huybrechts, D. R., Grobet, P. J., and Jacobs, P. A., Proceedings of the 9th International Congress on Catalysis(Phillips, M. J., and Ternan, M. Eds.), Vol 1, p. 420. The Chemical Institute of Canada, Canada, 1988.

22. Galich, P. N., Golubchenko, I. T., Gutyrya, V. S., Il'in, V. G., and Neimark, I. E., Ukr. Khim. Zh. **31**(11), 1117 (1965).

23. Hicks, R. F., Kelher, C. S., Savatsky, B. J., Hecker, W. C., and Bell, A. T., J. Catal. **71**, 216 (1981).

24. Dietz, W. A., J. Gas Chromatogr. **5**, 67 (1967).

25. Breck, D. W., "Zeolite Molecular Sieves." p. 611. Wiley, New York, 1984.

26. Jacobs, P. A., Tielen, M., and Uytterhoeven, J. B., J. Catal. **50**, 98 (1977).

27. Ward, J. W., J. Catal. **14**, 365 (1969).

28. Ward, J. W., J. Catal. **10**, 34 (1968).

29. Mirodatos, C., Pichat, P., and Barthomeuf, D., J. Phys. Chem. **80**(12), 1335 (1976).

30. Mirodatos, C., Kais, A. A., Vedrine, J. C., Pichat, P., and Barthomeuf, D., J. Phys. Chem. **80**(21), 2366 (1976).

31. Kakihana, M., Kotaka, M., and Okamoto, M., J. Phys. Chem. **87**, 2526 (1983).

32. Ward, J. W., J. Phys. Chem. **72**(12), 4211 (1968).

33. Bertsch, L. and Habgood, H. W., J. Phys. Chem. **67**, 1621 (1965).

34. King, S. T., and Garces, J. M., J. Catal. **104**, 59 (1987).

35. Peri, J. B., J. Phys. Chem. **79**(15), 1582 (1975).

36. Cunningham, J., and Hodnett, B. K., J. Chem. Soc. Faraday Trans. I **77**, 2777 (1981).

37. Tanabe, K., "Solid Acids and Bases." p. 50. Academic Press, New York, 1970.

Chapter 3
Nature of the Active Base Site

3.1 Introduction

The synthesis and partial characterization of alkali modified X and Y zeolites for use as base catalysts was presented in Chapter 2. From that work, it was shown that upon impregnation of CsNaX and CsNaY with identical loadings of cesium acetate, the acetone activity (activity of catalyst which manifested in the yield of acetone) of the CsNaY zeolite is an order of magnitude greater than that found for the CsNaX zeolite. Also, the propylene activity of the impregnated CsNaX zeolite is considerably higher than that observed from CsNaY, and as a result yields only a 62% selectivity to acetone. In contrast, virtually no propylene activity is found for the impregnated CsNaY zeolite and thus gives a 97% selectivity to acetone. This dissimilarity in activity between the identically prepared X and Y zeolites is not fully understood as yet. However, this behavior is not uncommon. Rode et al. (1,2) observed also a significant difference in activity between identically prepared rhodium X and Y zeolites for hydroformylation. On a surface area basis, the impregnated CsNaY zeolite shows an acetone activity which is comparable to that observed for MgO. This high activity and selectivity for the impregnated CsNaY zeolite is due to a base site formed by the decomposition products of the cesium acetate (Chapter 2).

The purpose of this work is to investigate the nature of the base site formed by the decomposition of cesium acetate in CsNaY.

3.2 Experimental

3.2.1 Materials and Preparation

The synthesis of NaY and the exchange procedure have been given elsewhere in Chapter 2. Cesium carbonate (99.9%) and isopropanol (99.5%) were obtained from Aldrich. Cesium oxide (Cs_2O) at 99% purity was obtained from AESAR. CO_2 (99.8%) and helium containing 1% CO_2 were obtained from AIRCO and used with no further purification.

3.2.2 Impregnation

In a similar manner to that described in Chapter 2, CsOH was impregnated onto silica gel and activated carbon at ~2.0wt%.

In Chapter 2, strong evidence is provided to suggest that cesium acetate is occluded into CsNaY by leaving the zeolite unrinsed after exchanging NaY with cesium acetate. Catalysts studied here which have been prepared by this technique will be specified as CsNaY-Ace-UR (unrinsed, acetate exchanged Y zeolites).

3.2.3 Analysis

ESR spectroscopy was performed on a Varian E3 spectrometer. Samples were heated in helium and sealed in quartz tubes.

3.2.4 Reactor and Procedure

The reactor and procedure used in this work are described in Chapter 2. For partial pressures of CO_2 below 0.16 torr, helium containing 1% CO_2 was introduced into the feed. For experiments requiring a partial pressure of 5 torr, CO_2 (99.8%) was used. In both cases, the carrier gas (helium) was reduced to maintain a constant partial pressure of isopropanol.

3.3 Results and Discussion

Several candidates for the active site generated by the decomposition of the cesium acetate in CsNaY are considered in this investigation. They are cesium metal, carbonate, hydroxide, and oxide. It should be noted that both the acetone and propylene activity of the CsNaY-Ace-UR zeolite are always highest at initial reaction times (see for example Fig. 5 of Chapter 2). We, therefore, assume that after calcination the active site is present before the onset of the reaction and is not formed as a result of contact with the reaction environment.

3.3.1 Cesium Metal

Sodium clusters in large pore zeolites were recently investigated by Martens et al. (3) by *in situ* ESR and IR spectroscopy. They suggested that framework oxygen anions in the neighborhood of neutral sodium clusters were the active base site. Wood et al. (4) investigated the decomposition of Cs_2CO_3 by Knudsen cell mass spectroscopy and observed cesium metal in the vapor phase. Garces et al. (5) postulated that similar behavior should be observed with KNaX, RbNaX, and CsNaX, and, in fact, detected K, Rb, and Cs metal vapor over these materials at temperatures above 327°C. In light of these observations, it seems plausible that cesium metal could form upon calcination of our impregnated CsNaY zeolite and may, therefore, promote the base catalyzed dehydrogenation of isopropanol.

To investigate the formation of cesium metal upon calcination of the modified CsNaY zeolite, ESR spectroscopy was employed. The CsNaY catalyst, impregnated at ~2.0 cesium acetate molecules per unit cell (~2.4wt%), was calcined at 550°C in helium. The sample temperature was then lowered to 77K for ESR analysis. Blazey et al. (6) studied alkali clusters in zeolite X and Y and concluded that these clusters are chemically stable at room temperature. Therefore, any clusters formed upon calcination in this study were expected to remain during the cooling for ESR analysis. No ESR signals were detected that could be assigned to either cesium metal or ionic clusters (6,7). From this result, we exclude cesium metal or charged clusters as the active site for isopropanol dehydrogenation.

3.3.2 Cesium Carbonate

Using infrared spectroscopy, carbonates have been identified on alkali-exchanged X zeolites (8,9). Carbonates were observed on CsNaY-Ace-UR zeolite as well (Figures 7 and 8 of Chapter 2). investigate the potential of the carbonate ions as the active species for the catalytic decomposition of isopropanol, bulk cesium carbonate was employed. Cesium carbonate (99^+%) was loaded into the reactor, heated to 350°C in flowing helium, and subjected to the reactant flow specified in Chapter 2. Only trace acetone was detected and no propylene was observed. To further analyze for the presence of carbonates after calcination an IR spectrum of the CsNaY-Ace-UR zeolite was recorded at 550°C in air using an *in situ* cell. No bands assignable to carbonate species were observed. Note that calcined (550°C) CsNaY-Ace-UR zeolite is active for acetone formation showing that the active site is present after calcination at 550°C. In light of these results, we exclude cesium carbonate as the active site.

3.3.3 Cesium Hydroxide

From activity results of Chapter 2, both the unrinsed cesium acetate and hydroxide exchanged Y zeolite showed higher activities than their rinsed analogs. Furthermore, strong evidence is given to suggest that unrinsed samples contain occluded alkali salts. One can speculate that the acetate and hydroxide in the unrinsed CsNaY zeolite are converted to an identical base site. An alternative explanation could be that the occluded cesium acetate may decompose to form a hydroxide and, therefore, show similar activity.

If CsOH in the CsNaY zeolite remains intact and serves as the active site, then we might expect supported hydroxide to be catalytically active in the decomposition of isopropanol. Therefore, cesium hydroxide was impregnated into both silica gel and activated carbon at ~2.0wt%. Both catalysts were first calcined at 450°C in helium and then subjected to start-up procedure 1 of Chapter 2 for reaction rate measurements. No activity was observed from the silica supported cesium and only trace acetone activity was found from the carbon supported cesium. Although one can not exclude the possibility that the CsOH supported on silica and carbon decomposes during calcination or exposure to the reaction environment, similar catalytic activity on the zeolite, silica, and carbon is expected if CsOH acts as the active site. Therefore, CsOH does not appear to be the active site.

3.3.4 Cesium Oxide

The possibility that upon decomposition of the cesium acetate, a cesium oxide forms is discussed. A first step is simply to test the catalytic properties of cesium oxide (denoted Cs_xO_y) for isopropanol decomposition. Because water readily reacts with Cs_xO_y to form CsOH, all efforts were made to minimize any exposure to water vapor prior to loading the reactor. Therefore, Cs_xO_y crystals were ground to a fine powder in a glove box. The powder was quickly transfered into the reactor which was being purged with helium. The reactor temperature was then elevated from room temperature to 350°C at ~4°C/min. At 350°C the oxide was subjected to the reaction environment specified in Chapter 2 and F/W at 0.98 mole isopropanol • hr^{-1} • g^{-1}. The initial yield of acetone from Cs_xO_y was 3.6% but slowly fell to 0.5% over 3 hours. Propylene activity was detectable at 5 minutes, but fell below the detection limits as the reaction proceeded.

The selectivity to acetone 5 minutes into the reaction was 99.1%. In light of these results, two points are important. First, the selectivity to acetone for CsNaY impregnated with ~2.0 cesium acetate molecules per unit cell is 97.4%. Second, the CsNaY-Ace-UR zeolite has very high initial activity, but also slowly falls to lower levels of conversion (Fig. 13). Owing to the similarity in both the start-up kinetics and high selectivity, it would appear that cesium oxide is a likely candidate for the active site formed by the decomposition of cesium acetate in CsNaY.

The decline in activity for the CsNaY-Ace-UR zeolite and Cs_xO_y is consistent with the behavior of other oxides as well. Several factors are attributed to the loss in activity such as site blockage by carbonate formation (10), or a reduction of the oxide surface by dehydroxylation (11). Another factor which could compliment site blockage or reduction could be a change in the order of the kinetics with site loss. Akiba et al. (12) showed that over ZnO, the initial isopropanol kinetics were second order but as the reaction proceeded, the kinetics convert to first order thus lowering activity. For the CsNaY-Ace-UR zeolite, the exact loss in activity is not clear. However, from our studies involving CO_2, a consumption of the active site by the reaction environment could explain the observed loss. As illustrated in Figure 13, it is noted that when the CsNaY-Ace-UR zeolite is contacted with CO_2, the base activity is quenched. However, upon removal of CO_2 from the feed, the high activity observed at initial times is re-established suggesting that the active base site is regenerated. Promotion of the base activity by CO_2 contact was shown also to occur in the synthesis of methanol over Cu/ZnO (13). In that study, Klier et al. (13) suggested that CO_2 may act as an oxidizing agent which oxidizes sites reduced by the reaction environment. CO_2 was reported also to reactivate the activity for methane coupling over Li/MgO (14). Korf et al. (14) suggested that the lithium reacts with the CO_2 to form a carbonate which then decomposed to the active site.

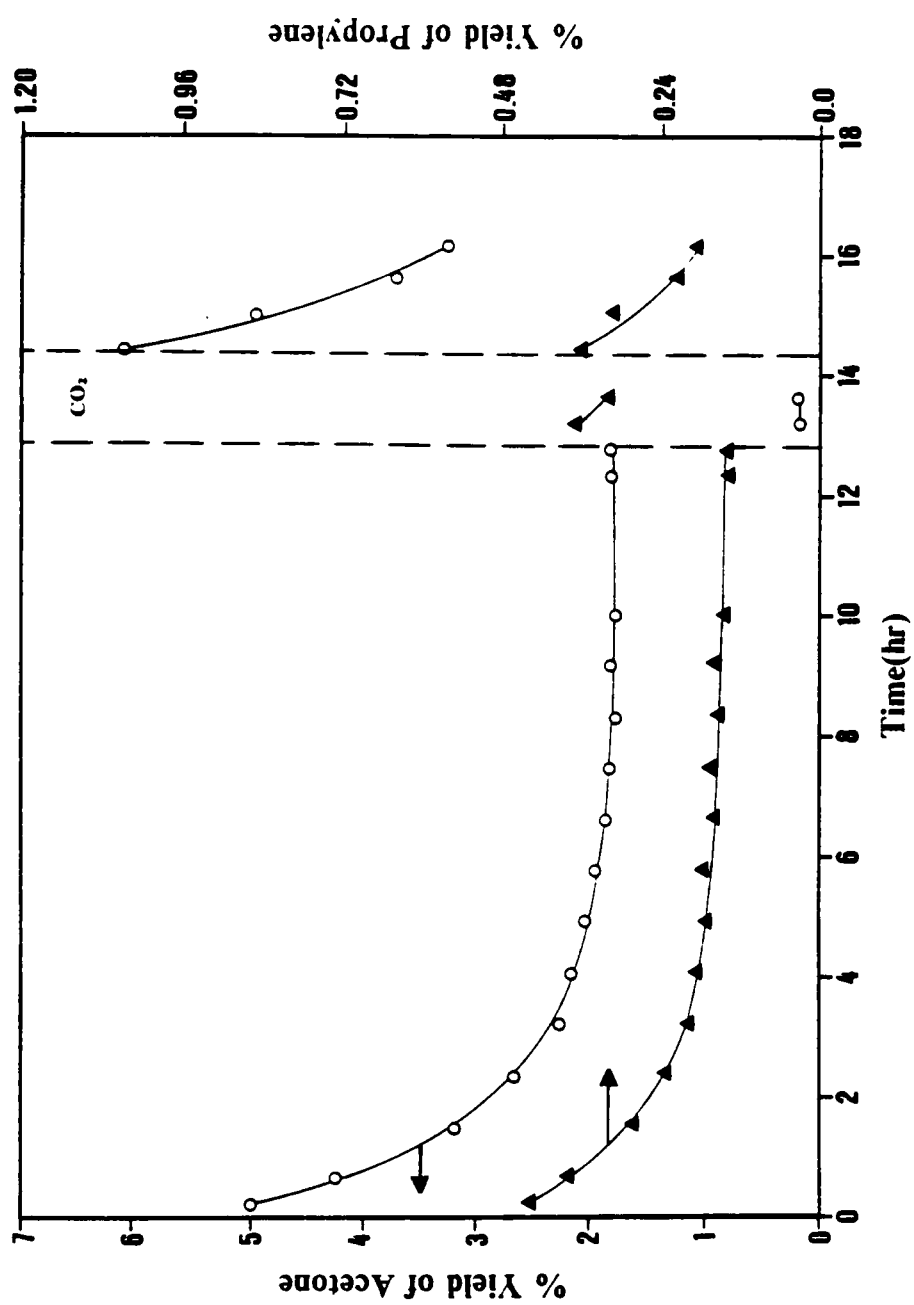

Figure 13 Influence of CO_2 Contact on Activity of CsNaY-Ace-UR Zeolite. ○ ,acetone; ▲ , propylene. F/W = 2.41 mol isopropanol • hr^{-1} • g, temperature = 350°C, total pressure = 1 atm., and partial pressure of isopropanol = 152 torr(STP). Start-up procedure 2.

Further evidence which supports the case for cesium oxide as the active site is provided by the activity data obtained with the different calcination atmospheres (Chapter 2). The CsNaY-Ace-UR zeolite was calcined in both an oxygen (99.5%) and a helium (99.995%) atmosphere at 500°C to investigate the effect of O_2 on the decomposition of the cesium acetate. By exposing the CsNaY-Ace-UR zeolite to such an oxidizing atmosphere it is expect that an oxide will result from the decomposition of cesium acetate. The results listed in Table 2D of Chapter 2 show that the catalytic activity for formation of acetone and propylene is, in fact, higher when the catalyst is calcined in oxygen compared to helium. However, the calcination atmosphere has little effect on selectivity which may suggest that the cesium acetate decomposition products are similar for both atmospheres, but the oxygen atmosphere is more effective in generating the active site.

Another characteristic of metal oxides is their ability to dehydrate alcohols over base sites. It has been shown that alcohols can dissociatively adsorb on metal oxides to form alkoxides (15-17). These alkoxides have been suggested to decompose further to form dehydrogenation products (ketones/aldehydes) or dehydration products (olefins) (11,18-21). We might, therefore, expect the loss in acetone activity to be paralleled by a loss in propylene activity if, in fact, an alkoxide is the reaction intermediate. Figure 13 shows the acetone and propylene activity before and after CO_2 contact. The results show that the high acetone activity is paralleled by the propylene activity both before and after CO_2 contact. Furthermore, the selectivity to acetone before and after CO_2 contact never deviated more than 0.43% and 0.18%, respectively.

If it is assumed that a isopropoxide intermediate exists on the CsNaY-Ace-UR zeolite during the reaction, then both the acetone and propylene activity could possibly be poisoned by an electrophilic adsorbate. MgO, which was suggested to adsorb alcohols dissociatively to form alkoxides (17,19,23), was contacted with CO_2 at a partial pressure of *ca.* 5 torr in an attempt to poison both the acetone and propylene activity.

As illustrated in Figure 14, both the acetone and the propylene activity of MgO are poisoned upon exposure to CO_2. With removal of the CO_2 from the feed stream, the acetone and propylene activity recover immediately to their steady state activities. For the CsNaY-Ace-UR zeolite (Fig. 13), the acetone activity was suppressed upon CO_2 contact, however, the propylene activity was promoted. This promotion in propylene activity upon CO_2 contact has been observed elsewhere (24-26). Frilette and Munns (24) showed that the propylene activity over NaX increases with increasing partial pressures of CO_2. Mirodatos et al. (25,26) suggested from infrared studies on various forms of zeolite Y that CO_2 reacts with hydroxylated divalent cations to form carbonate species and new acidic H^+ sites. Therefore, the possibility exists that any loss in propylene activity associated with the poisoning of a propoxide intermediate via CO_2 could be overshadowed by other types of promotion in propylene activity. In an attempt to circumvent this problem, very low partial pressures of CO_2 were used in order to minimize the possible promotion of propylene activity. Thus, any loss in propylene activity associated with the propoxide decomposition could more likely be observed. Figure 15 shows that with increasing partial pressures of CO_2 both the acetone and propylene activity are suppressed. Selectivity remained at 96.8%$\pm$0.18% for P/Po below 11 X 10^{-5} suggesting that some of the observed propylene activity was resulting from a propoxide intermediate.

3.4 Conclusions

From the results presented in this work, it appears that the active site formed by the decomposition of the cesium acetate in CsNaY is cesium oxide. No evidence is found to

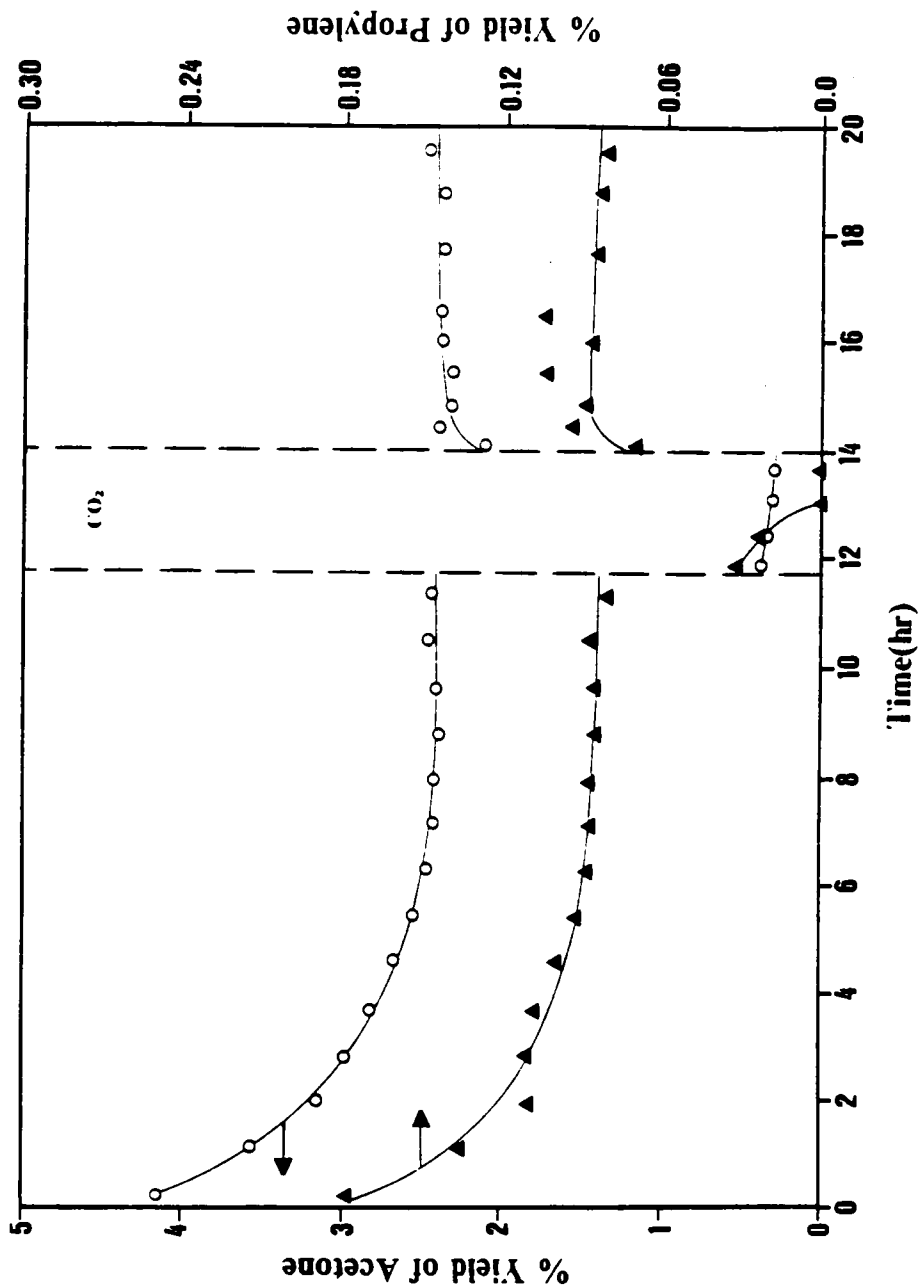

Figure 14 Influence of CO_2 Contact on Activity of MgO. ○, acetone; ▲, propylene. F/W = 1.07 mol isopropanol • hr^{-1} • g^{-1}, temperature = 350°C, total pressure = 1 atm., and partial pressure of isopropanol = 152 torr(STP). Start-up procedure 2.

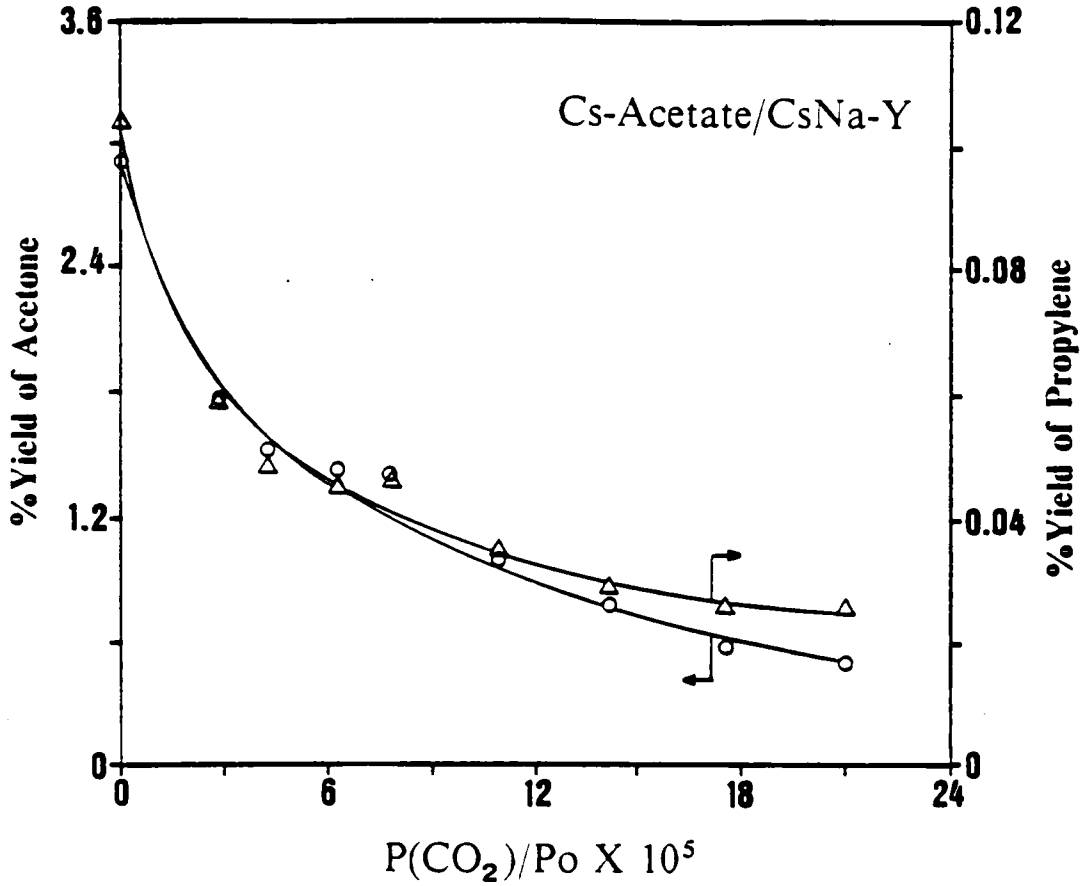

Figure 15 Influence of CO_2 Contact at Low Partial Pressures of CO_2 on Activity of the CsNaY-Ace-UR Zeolite. ○ , acetone; △ , propylene. F/W = 6.53 mol isopropanol• hr^{-1} • g^{-1}, temperature = 350°C, total pressure = 1 atm., and partial pressure of isopropanol = 152 torr(STP).

suggest that after calcination the final decomposition products of cesium acetate are cesium metal, carbonate, or hydroxide. The results suggest also that a portion of the propylene activity may be resulting from a propoxide intermediate.

3.5 *References*

1. Rode, E. J., Davis, M. E., Hanson, B. E., J. Catal. **96**, 563 (1985).
2. Rode, E. J., Davis, M. E., Hanson, B. E., J. Catal. **96**, 574 (1985).
3. Martens, L. R., Vermeiren, W. J., Huybrechts, D., R., Grobet, P. J., and Jacobs, P. A., Proceedings of the 9th International Congress on Catalysis(Phillips, M. J., and Ternan, M., Eds.), Vol. 1, p. 420. The Chemical Institute of Canada, Canada, 1988.
4. Wood, B. J., Brittain, R. D., and Lau, K. H., Am. Chem. Soc., Div. Fuel Chem. **28**(1), 55 (1983).
5. Garces, J. M., Vrieland, G. E., Bates, S. I., Scheidt, F. M., in "Catalysis by Acids and Bases"(B. Imelik et al., Eds.), Vol. 20, p. 67. Elsevier, Amsterdam, 1985.
6. Blazey, K. W., Muller, K. A., Blatter, F., and Schumacher, E., Europhys. Lett. **4**(7), 857 (1987).
7. Smeulders, J. B. A. F., Hefni, M. A., Klaassen, A. A. K., de Boer, E., Westphal, U. and Geismar, G., Zeolite **7**(4), 347 (1987).
8. King, S. T., and Garces, J. M., J. Catal. **104**, 59 (1987).
9. Bertsch, L., and Habgood, H. W., J. Phys. Chem. **67**, 1621 (1963).
10. Cunningham, J., and Hodnett, B. K., J. Chem. Soc. Faraday Trans. I **77**, 2777 (1981).
11. Kim, K. S., Barteau, M. A., and Farneth, W. E., Langmuir **4**, 533 (1988).
12. Akiba, E., Mitsuyuki, S., Takaharu, O., and Tamaru, K., Z. Phys. Chem. **119**, 103 (1980).
13. Klier, K., Chatikavanij, V., Herman, R. G., and Simmons, G. W., J. Catal. **74**, 343 (1982).
14. Korf, S. J., Roos, J. A., de Bruijn, N. A., van Ommen, J. G., and Ross, J. R. H., J. Chem. Soc., Chem. Commun., 1433 (1987).
15. Zaki, M. I., and Sheppard, N., J. Catal. **80**, 114 (1983).
16. Miyata, H., Wakamiya, M., and Kubokawa, Y., J. Catal. 34, 117 (1974).
17. Koga, O., Onishi, T. and Tamaru, K., J. Chem. Soc. Faraday Trans. I **76**, 19 (1980).
18. Parrott, S. L., Rodgers, Jr., J. W., and White, J. M., Appl. Surf. Sci. 1, 443 (1978).
19. Bowker, M., Petts, R. W., and Waugh, K. C., J. Chem. Soc. Faraday Trans. I **81**, 3073 (1985).
20. Bowker, M., Petts, R. W., and Waugh, K. C., J. Catal. **99**, 53 (1986).

21. Waugh, K. C., Bowker, M., Petts, R. W., Vandervell, H. D., and O'Malley, J., Appl. Catal. **25**, 121 (1986).

22. Martinez, R., and Barteau, M. A., Langmuir **1**(6), 684 (1985).

23. Frilette, V. J., and Munns, Jr., G. W., J. Catal. **4**, 504 (1965).

24. Mirodatos, C., Pichat, P., and Barthomeuf, D., J. Phys. Chem. **80**(12), 1335 (1976).

25. Mirodatos, C., Kais, A. A., Vedrine, J. C., Pichat, P., and Barthomeuf, D., J. Phys. Chem. **80**(21), 2366 (1976).

Chapter 4
Alkylation with Methanol

4.1 Abstract

Chapters 2 and 3 have delt with the development and characterization of a novel base zeolite. It is of interest in this chapter to apply this catalyst to the alkylation of toluene, ethane, methane, and acetone with methanol.

Ion exchanged CsNaX and CsNaY, cesium acetate impregnated CsNaX (CsAce/CsNaX) and CsNaY (CsAce/CsNaY), and MgO have been reacted with isopropanol at 425°C and atmospheric pressure to assess their acid/base properties at a temperature consistent with that used in the side chain alkylation of toluene with methanol. The results suggest the basic character of the catalysts tested follows the order:

$$MgO > CsAce/CsNaY > CsAce/CsNaX \simeq CsNaY > CsNaX$$

Selectivities to acetone measured at 4.73% conversion follows this order as well, ranging from 95.7% and 93.9% for MgO and CsAce/CsNaY, respectively, to 17.6% for the CsNaX. Thus, these catalysts can be group into two categories; (i) catalysts which vary in acid/base properties yet possess identical topology (e.g., the zeolites) and (ii) catalysts

which vary in topology yet have similar acid/base properties (e.g., MgO and CsAce/CsNaY). These catalysts were compared using the side chain alkylation of toluene, ethane, methane, and acetone with methanol. For the impregnated zeolites, similar toluene conversions were observed. Unlike the impregnated X zeolite no formaldehyde (i.e., the alkylating agent) was observed in the product stream of the impregnated Y zeolite. Both MgO and CsAce/CsNaY had similar methanol decomposition products, i.e, no formaldehyde and high CO formation, yet unlike CsAce/CsNaY no toluene conversion was observed for MgO. No conversion of ethane or methane was observed for either impregnated zeolite at 425°C. Attempts at higher temperatures (e.g., 465°C) failed also. Acetone was alkylated to methylvinylketone and methylethylketone over the impregnated zeolites. However, the majority of the reacted acetone formed products which appear to result from acetone aldol condensations.

4.2 *Introduction*

Chapters 2 and 3 describe the development and characterization of alkali modified zeolites as base catalysts. It was shown that impregnation of CsNaY with cesium acetate (CsAce/CsNaY) improved the intrinsic rate of isopropanol decomposition to acetone at 350°C by an order of magnitude above that observed from the untreated CsNaY zeolite. However, upon impregnation of the CsNaX zeolite with cesium acetate (CsAce/CsNaX) promoted the acetone activity only slightly above that of the untreated CsNaX zeolite and was comparable to the rate obtained from the untreated CsNaY zeolite. Furthermore, the selectivities to acetone were 97.4% and 61.6% for the CsAce/CsNaY and CsAce/CsNaX zeolite, respectively. When the rates of acetone formation were normalized per unit area, MgO and CsAce/CsNaY gave equivalent values. Studies aimed at elucidating the nature of the active site on CsAce/CsNaY (Chapter 3) suggested that the cesium acetate decomposed to form cesium oxide, and it is the oxide which was suspect to be the active site for acetone formation. Evidence was presented also to indicate the presence of an isopropoxide intermediate which was responsible for the minor amounts of propylene formed over the CsAce/CsNaY catalyst. Thus, the CsAce/CsNaY catalyst possessed (i) significantly higher activity for the production of acetone from isopropanol (normally attributed to base sites), and (ii) virtually no Bronstëd acid sites.

The alkylation of toluene with methanol has been studied extensively over a variety of catalysts(1-7). Figure 16 provides a general reaction scheme for the acid (xylenes) and base (styrene) catalyzed routes. It is generally accepted that in the side chain alkylation of toluene, methanol is dehydrogenated to formaldehyde and it is the formaldehyde which serves as the alkylating agent to form styrene by an aldol-type reaction. Note that

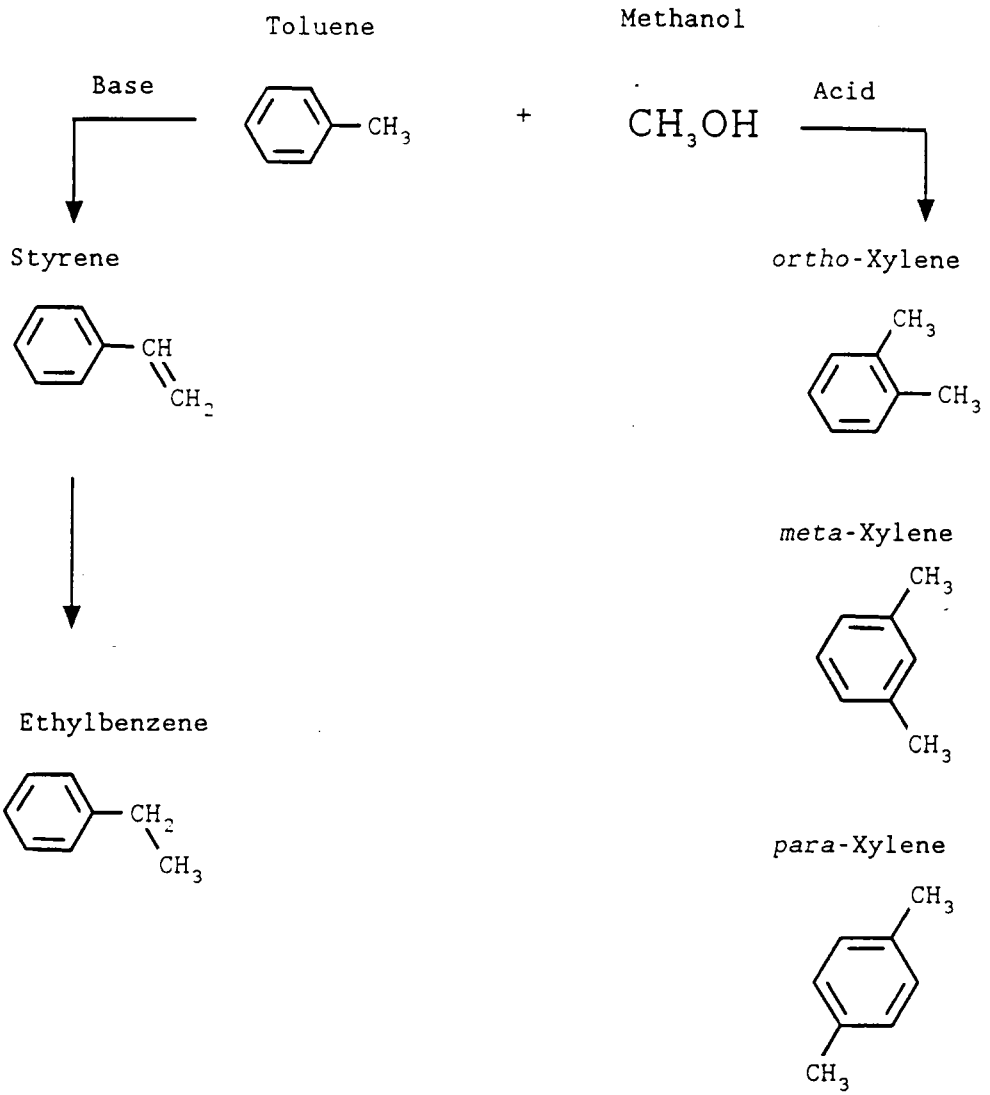

Figure 16 Reaction Scheme for Toluene Alkylation with Methanol.

an undesirable side reaction is the hydrogenation of styrene to ethylbenzene. CsNaX zeolites impregnated with boric acid(3,7) and/or copper nitrate (8) appear to be the most effective catalysts for the side chain alkylation. Several factors have been suggested to play important role for side chain alkylation to occur and they are (i) active base sites, (ii) spatial constraints found within the zeolite pores, and (iii) stabilization of the formaldehyde. Although considerable evidence is available to show that strong acid sites can result in ring alkylation to xylene (2,5,9,10), a certain degree of acidity is thought to promote the stability of the formaldehyde (7,11).

The objective of this work is to study the alkylation of toluene, acetone, ethane, and methane with methanol using the novel, base catalyst we developed previously in Chapters 2 and 3, i.e., CsAce/CsNaY, and to make a direct comparison between the alkylation results and those obtained from isopropanol decomposition.

4.3 Experimental

4.3.1 Materials

The synthesis of zeolites X and Y and the ion exchange procedures used have been previously described in Chapter 2. After exchange, the CsNaX and CsNaY zeolites were rinsed with deionized water to remove the possibility of salt occlusion. The materials were then dried at 100°C. These solids will be denoted as untreated CsNaX and CsNaY. Magnesium oxide was formed by the *in situ* dehydroxylation of $Mg(OH)_2$ in helium at 550°C. Isopropanol, toluene, acetone, and methanol were purchased from Aldrich and

possessed purities greater than 99.9%. Ethane, methane, and helium were obtained from Airco at greater than 99.9%.

4.3.2 Impregnation

Prior to impregnation the exchanged solids were rinsed with 0.01N cesium acetate to remove the possibility of salt occlusion yet minimize decationation. Impregnation of cesium acetate was accomplished by micropipetting 0.025N cesium acetate into a round bottom flask. Subsequently, the dried acetate rinsed CsNaY or CsNaX was added so that a precalculated loading (~2.5 cesium acetate molecules per unit cell or 2.8wt% for CsNaY) could be achieve upon removal of the water. The flask was mounted onto a rotovap and rotated for ~8 hours at 25°C and 1 atmosphere. Finally, vacuum was applied and the temperature elevated to 40°C to remove bulk water and leave the cesium acetate occluded in the zeolites (*vide infra*).

4.3.3 Analysis

Thermogravimetric analyses (TGA) were performed on a Dupont 951 thermogravimetric analyzer. Argon adsorption isotherms were obtained using the Omnisorp 100 system developed by Omicron Technology. Superficial (i.e., < ~50Å) analyses of the zeolites for silicon (Si_{2_p}) and cesium (Cs_{3_d}) where performed by X-ray photoelectron spectroscopy (XPS) with a Perkin-Elmer Phi 5300 ESCA which employed a Mg Kα X-ray source. Several bulk chemical analyses of the zeolites for Si and Cs were obtained from Galbraith Laboratories, Inc. (Knoxville, TN) while other zeolite samples

were analyzed for cesium, sodium, and aluminum on a Jarrell-Ash 9000 Inductively Coupled Argon Plasma Spectrometer.

4.3.4 Reactor System

Liquid reactants were fed by a syringe pump into a 160°C constant temperature vaporizer where they were mixed with either gas phase reactants and/or helium. The heated stream was able to bypass or feed into a vertical, down flow, fixed bed microreactor. For isopropanol decomposition, the microreactor consisted of a 3mm i.d. vycor tube placed inside a tube furnace. Alkylation experiments required larger loadings of catalyst and a 10mm i.d. quartz tube was employed. During the alkylation runs, two thermocouples located at the center of the catalyst bed and at the outside wall of the quartz tube were used to monitor the temperature. A temperature gradient of ~ 10°C was typically observed, and the temperature reported here are the averages. Isopropanol decomposition products were monitored by online gas chromatography. During alkylation, products were monitored by gas chromatography by injection of liquid samples (collected by a liquid nitrogen trap) and by injection from an online gas sampling valve.

4.3.5 Procedure

The catalysts were compacted without binder into pellets. These pellets were crushed and size separated to -60/+80 mesh (isopropanol decomposition) or -35/+60 mesh (alkylation). As in Chapter 2, contact times are based upon the number of zeolite unit

cells rather than weight. MgO is compared to CsAce/CsNaY on the basis of surface area. MgO and the impregnated CsNaY have BET surface areas of 125 and 492 m^2/g, respectively.

The conditions used for isopropanol decomposition studies are: isopropanol and helium flow rates of 45 and 180 cc (STP) per minute, respectively, T = 425°C, and W/F = 6.1 X 10^{-6} mole zeolite unit cell • h • (mole isopropanol)$^{-1}$. For the comparison between MgO and CsAce/CsNaY, W/F = 52.0 m^2 • h • (mole isopropanol)$^{-1}$. Note that the contact time used for MgO is identical to that used previously for CsAce/CsNaY in isopropanol decomposition when normalized to a surface area basis. The yields and selectivities reported here for isopropanol decomposition runs are defined as: y_i = moles of *i* formed per mole isopropanol fed times 100%, s_i = moles *i* formed per mole isopropanol reacted times 100%, were *i* represents either acetone or propylene.

For the alkylation of toluene, acetone, ethane, and methane, the substrate-to-methanol ratio is 5, the helium-to-reactant ratio is 5, and the reaction temperature varied from 380 to 465°C. The substrate and methanol flow rates are were 12.8 and 2.6 cc (STP) per minute, respectively, and W/F = 1.45 X 10^{-3} mole zeolite unit cells • h • (moles of substrate plus methanol)$^{-1}$. For the comparison between MgO and CsAce/CsNaY, W/F = 1.23 X 10^4 m^2 • h • (moles of substrate plus methanol)$^{-1}$. The contact time used for MgO is identical to that used by CsACe/CsNaY in alkylation when normalized to a basis of surface area. Conversions, yields , and selectivities are defined as: C_s = moles of substrate reacted per mole substrate fed times 100%, Y_i = moles *i* formed per mole substrate fed times 100% where *i* is the alkylated product. For the methanol decomposition products, yields are defined as: Y_i = moles of *i* formed per mole of methanol fed times 100% where *i* represents either CO, CO_2, dimethylether (DME), or formaldehyde. The production of H_2 was not monitored.

4.4 Results

The Si/Al ratio, the percent exchange, and the molecular weight per unit cell of the untreated zeolites were determined from bulk chemical analysis and are listed in Table 4. Because of the low levels of impregnation (approximately 2.5 cesium acetate molecules per unit cell) the difference in molecular weight between the untreated and impregnated zeolites is assumed to be 480 gm/gmole or 2.5 times the formula weight of cesium acetate (approximate verification was obtained by monitoring the weight loss from the combustion of the acetate molecules by TGA).

Figure 17 shows the acetone and propylene yields obtained from the untreated and impregnated CsNaY and CsNaX zeolites at 425°C and constant W/F. For the X catalysts, an increase in acetone yield from 0.46% to 1.05% was observed with impregnation. Furthermore, the propylene yield fell from 3.29% to 1.46%. The impregnation of CsNaY proved to be far more effective in promoting the yield of acetone and is consistent with the results of Chapters 2 and 3. For the untreated and impregnated CsNaY zeolite, the acetone yield was 0.92% and 4.33%, respectively. As was observed for the X zeolite, propylene yields declined as a result of impregnation (1.05% to 0.28%).

Figure 18 illustrates the selectivity to acetone at 425°C and constant conversion for both the untreated and impregnated zeolites at an isopropanol conversion of 4.73%. The selectivity to acetone increases from 17.6% for the untreated CsNaX zeolite to 93.9% for the impregnated CsNaY zeolite.

At a constant W/F (surface area basis), the yield of acetone for MgO is 9.12% while that for CsAce/CsNaY is 4.73%. The yields of propylene are similar at 0.37% and 0.28% for MgO and CsAce/CsNaY, respectively, while selectivities to acetone at a conversion of 4.73% are 93.9% and 95.7%, respectively.

Table 4. Physical Data of Zeolite Catalysts for Alkylation with Methanol.

Catalyst	Si/Al	% Exchanged[a,b]	Molecular Wt. per unit cell[c]	Cesium acetate per unit cell
CsNaX	1.34	60	18710	-
CsAcc/CsNaX	1.34	60	19190	~2.5
CsNaY	2.34	64	16870	-
CsAcc/CsNaY	2.34	64	17350	~2.5

a) Based on a unit cell composition of: NaY: $Na_{58}Al_{58}Si_{134}O_{384}$
NaX: $Na_{82}Al_{82}Si_{110}O_{384}$

b) Exchange via acetate

c) Dehydrated

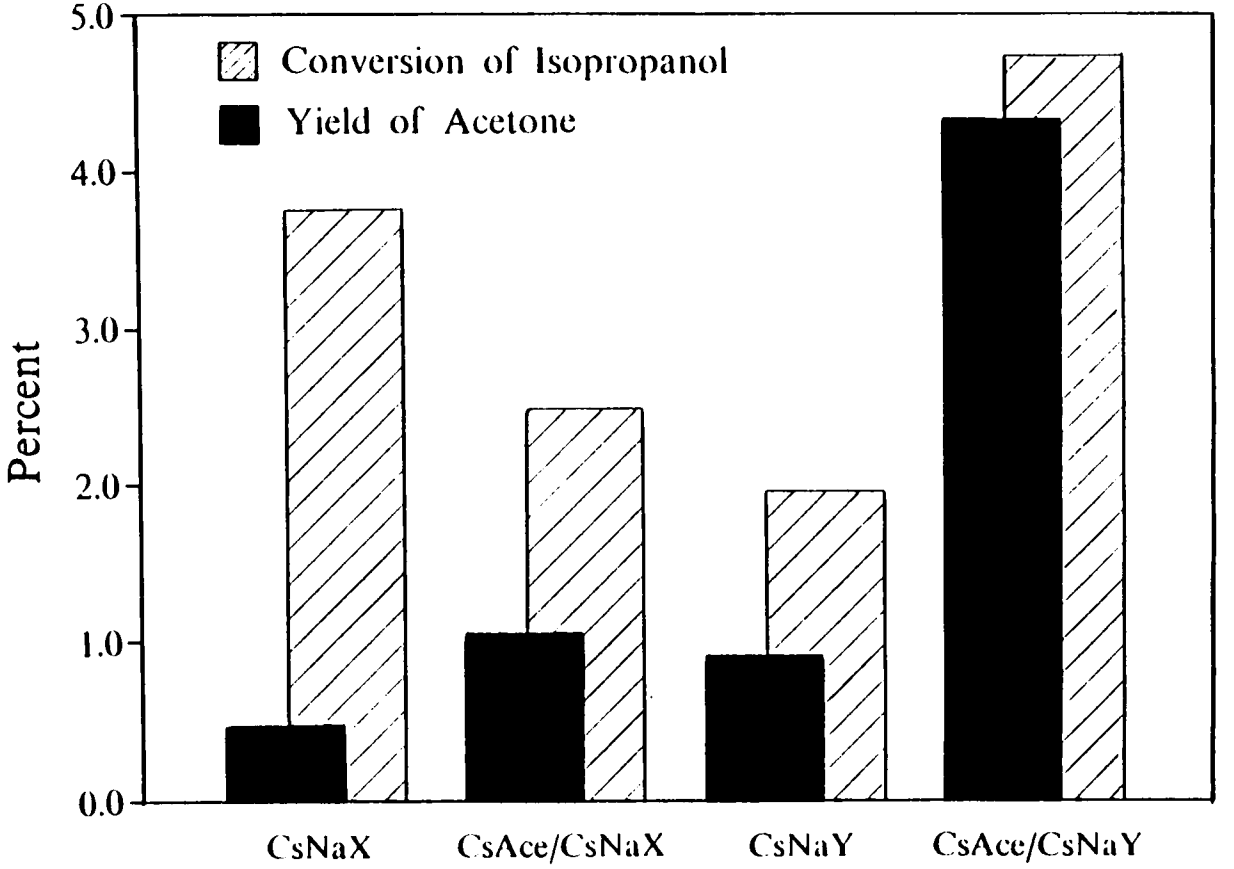

Figure 17 Conversions of Isopropanol and Yields of Acetone at Constant Contact Time. W/F = 6.13 X 10^{-6} mole zeolite unit cell • h • (mol isopropanol)$^{-1}$, temperature = 425°C, total pressure = 1 atm., and partial pressure of isopropanol = 152 torr.

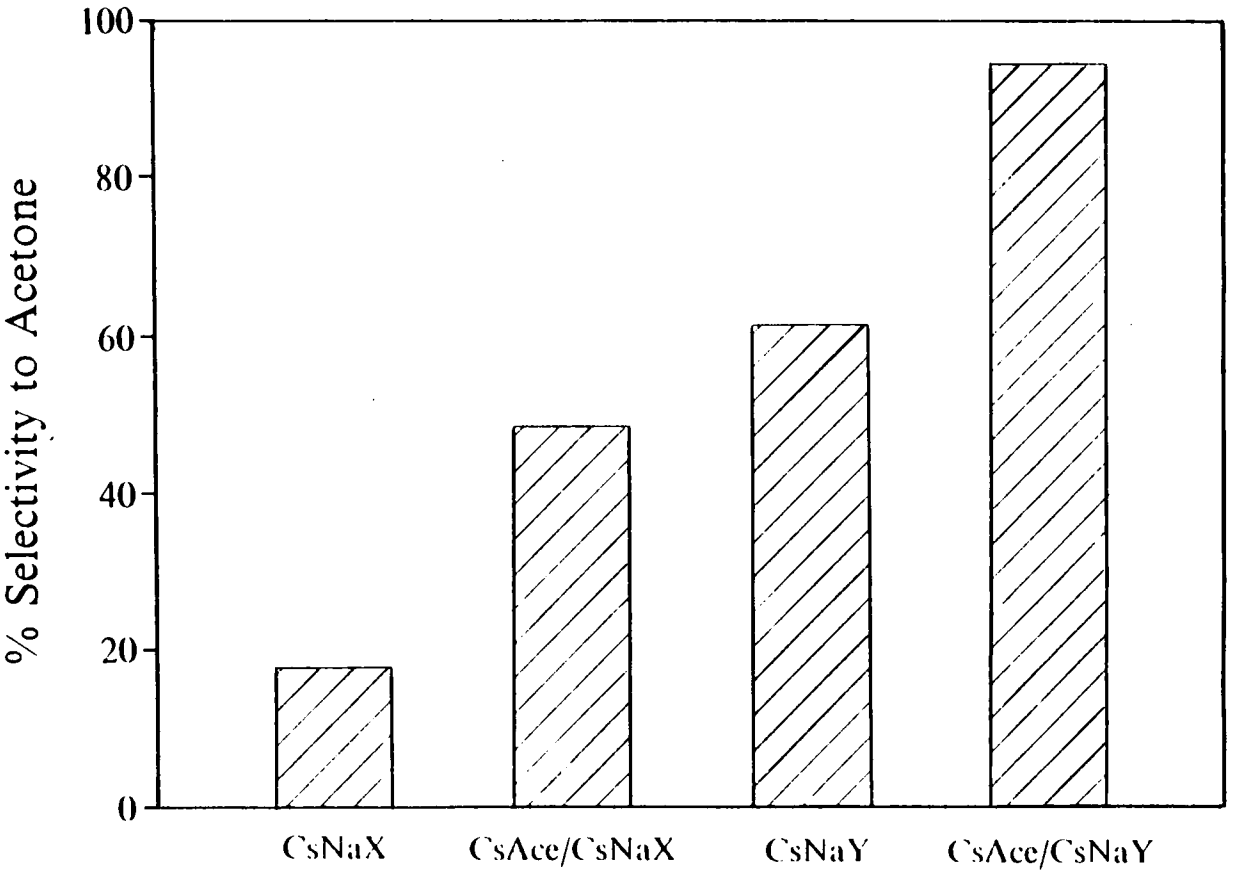

Figure 18 Selectivity to Acetone at Constant Isopropanol Conversion. Conversion = 4.73%, temperature = 425°C, total pressure = 1 atm., and partial pressure of isopropanol = 152 torr.

Figure 19 shows the conversions of toluene and yields of styrene from the untreated and impregnated zeolites at a constant W/F and at a reaction temperature of 437°C. For both impregnated X and Y zeolites, a significant increase in toluene conversion is observed. Furthermore, trace amounts of xylenes are observed only from the untreated CsNaY catalyst.

Figure 20 shows the influence of the reaction temperature on the toluene conversion. As observed in Figure 19, the conversion of toluene is slightly higher for CsAce/CsNaY than CsAce/CsNaX. For both zeolites, the toluene conversion obtains a maximum at 425-435°C. Figures 21A and 21B illustrate the yields of methanol decomposition products during toluene alkylation for the impregnated zeolites as a function of temperature. For CsAce/CsNaX zeolite, dimethylether (DME) and formaldehyde are observed in the product stream. For the CsAce/CsNaY zeolite, only trace amounts of formaldehyde and DME are observed. Figure 21B shows the yield of CO for CsAce/CsNaY and CsAce/CsNaX. For all temperatures, the yield of CO from CsAce/CsNaY is significantly higher than that obtained from CsAce/CsNaX. CO_2 yields (not shown) are fairly similar for both zeolite and range from ~ 0.15% at 380°C to ~1.3% at 465°C.

Table 5 lists the conversions of toluene and methanol at 425°C for the impregnated zeolites and MgO. Listed also are the product yields from toluene and methanol. Note that MgO did not convert toluene. Interestingly, MgO and CsAce/CSNaY show similar methanol decomposition products. Only trace formaldehyde and DME are observed over these catalysts and both exhibit high CO formation.

The alkylation of acetone, ethane, and methane with methanol was studied over the impregnated X and Y zeolites at a W/F identical to that used for the alkylation of toluene. Table 6 lists the conversion of substrate and methanol. No conversion is observed either for methane or ethane. At higher temperatures (e.g., 465°C) ethane and

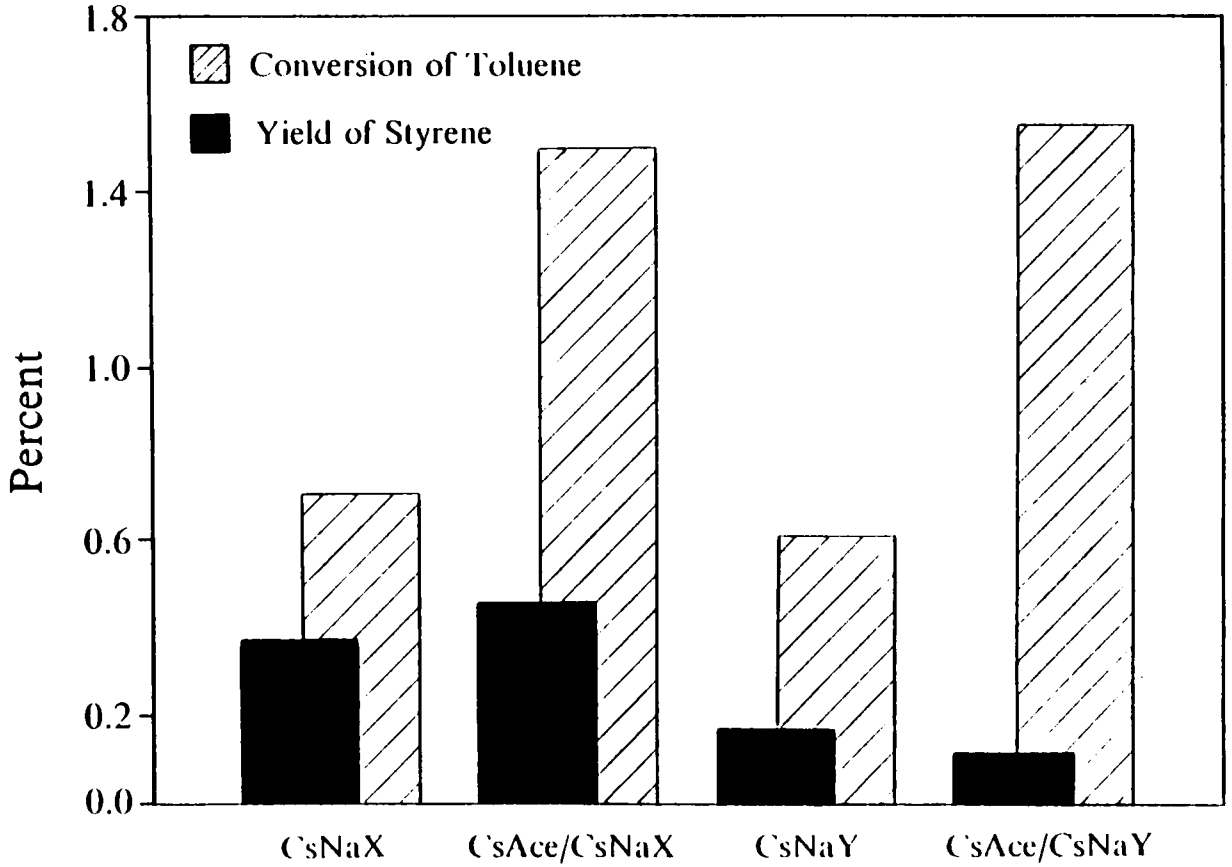

Figure 19 Influence of Catalyst on Toluene Conversion and Styrene Yield. W/F = 1.45 X 10 ^{3} mole zeolite unit cell • h • (moles of toluene + methanol) $^{-1}$, temperature = 437 °C, total pressure = 1 atm., toluene/methanol = 5, helium/(toluene + methanol) = 5.

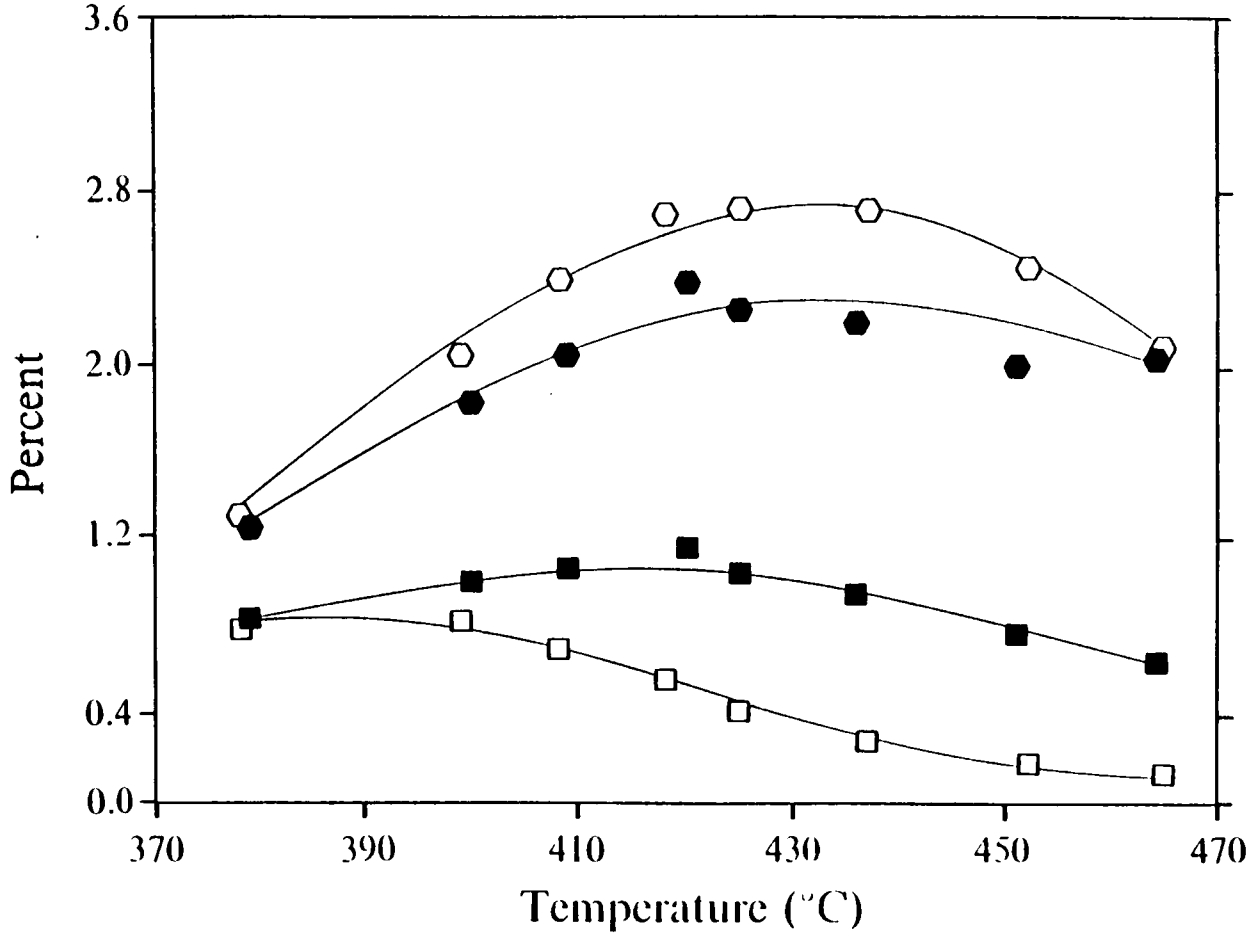

Figure 20 Temperature Dependence on Toluene Conversion and Styrene Yield. Toluene conversion: ⬢, CsAce/CsNaX; ⬡, CsAce/CsNaY. Styrene yield: ■, CsAce/CsNaX; □, CsAce/CsNaY. W/F = 1.45 X 10 ^{3} mole zeolite unit cell • h • (moles of toluene + methanol)$^{-1}$, total pressure = 1 atm., toluene/methanol = 5, helium/(toluene + methanol) = 5.

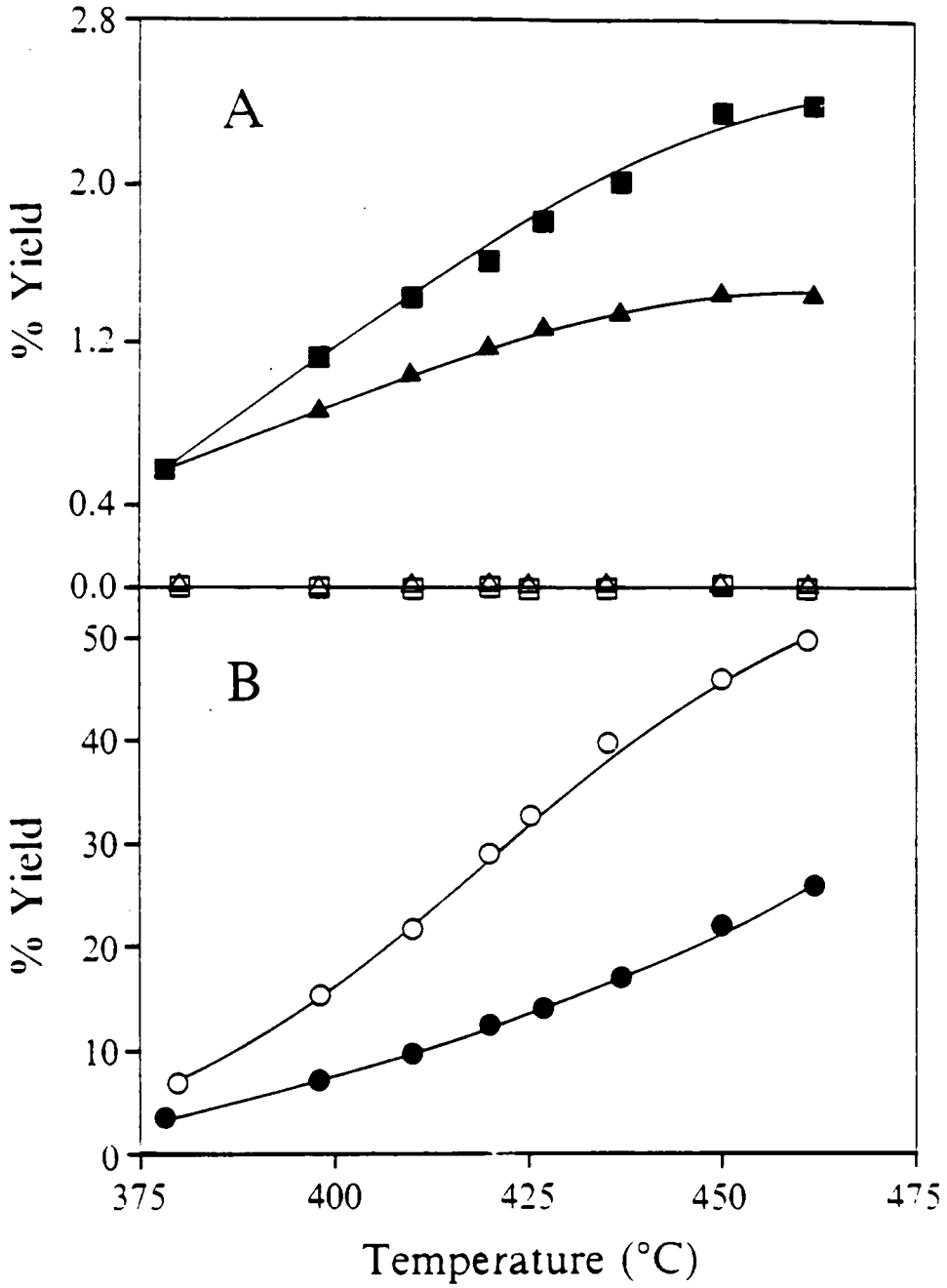

Figure 21 Influence of Temperature on Decomposition of Methanol. (A) Formaldehyde yield from: ▲, CsAce/CsNaX; △, CsACe/CSNaY. DME yield from: ■, CsAce/CSNaX; □, CsAce/CsNaY. (B) CO yield from: ●, CsACe/CSNaX; ○, CsAce/CsNaY. W/F = 1.45 X 10^{-3} mole zeolite unit cell • h • (moles of toluene + methanol)$^{-1}$, total pressure = 1 atm., toluene/methanol = 5, helium/(toluene + methanol) = 5.

Table 5. Toluene Alkylation with Methanol: Conversions and Yields at 425°C.

	Reactants		Products						
Catalyst	Conversion of Toluene	Conversion of Methanol	Yield of Styrene	Yield of EB	Yield of xylenes	Yield of CO	Yield of CO_2	Yield of CH_2O	Yield of DME
CsAce/CsNa-X	2.27	33.4	1.07	1.07	0	14.4	0.97	1.28	1.81
CsAce/CsNa-Y	2.74	54.3	0.43	2.29	0	33.0	0.49	*trace*	*trace*
MgO	0.0	32.8	0	0	0	28.0	0.36	*trace*	*trace*

Table 6. Substrate Alkylation with Methanol at 425°C.

Substrate	C-H Acidity[a] Approx. pK_a	CsAcc/CsNa-Y % Conv. Substrate	CsAcc/CsNa-Y % Conv. Methanol	CsAcc/CsNa-X %Conv. Substrate	CsAcc/CsNa-X % Conv. Methanol
Acetone	20	5.81[b]	39.1	7.83[b]	37.2
Toluene	35	2.74	54.3	2.24	33.4
Methane	40	0.0	72.7	0.0	42.4
Ethane	42	0.0	89.9	0.0	53.4

a) From ref (30).

b) Yields of methylvinylketone plus methlyethylketone were 0.26% and 0.23% for CsAce/CsNaY and CsAce/CsNaX, respectively.

methane remain unreacted. Alkylation of acetone with methanol was observed over both catalysts at 425°C. However, the majority of the reacted acetone formed products which appear to result from acetone aldol condensations.

Table 7 gives the superficial and bulk chemical analyses of cesium and silicon for the CsNaY and CsAce/CsNaY catalysts. Included in Table 7 are analogous data from rhodium containing zeolite A and Y catalysts which will be used for comparative purposes (*vide infra*).

4.5 Discussion

4.5.1 Acid/Base Properties

In the decomposition of isopropanol to acetone and propylene the acid/base properties are typically based on the rate and selectivity of acetone and propylene production. Although some ambiguity can exist as to whether propylene results from a Bronstëd acid site(12,13) or from the decomposition of an alkoxide intermediate (14-19) the production of acetone is fairly well accepted to result from base sites (14-19). Because activity and selectivity can be strongly influence by temperature it was necessary to determine whether conclusions obtained at 350°C in Chapter 2 were valid also at temperatures consistent with those used for the side chain alkylation of toluene with methanol. From Figure 20 the optimum temperature for toluene conversion ranges between 425 and 435°C for both CsAce/CsNaX and CsAce/CsNaY. This range is within those reported earlier (2,4). Thus, isopropanol decomposition studies were performed at 425°C. To

Table 7. Superficial and Bulk Chemical Analyses of Zeolite Catalysts.

Catalyst	Loading Weight%	Metal/Si		XPS/CA
		CA	XPS	
CsNa-Y	0.0 Cs^+	0.33	0.38	1.15
CsAcc/CsNa-Y	1.95 Cs^+	0.37	0.45	1.22
$RhCl_3$/Na-A[a]	1.25 Rh^{3+}	0.02	1.33	60
RhNaY[a]	2.37 Rh^{3+}	0.023	0.023	1.0

a) From ref. (27).

assess the relative activity of each catalyst, i.e., yield of acetone and propylene, all catalysts were compared at a constant contact time (Figure 17). The conversions of isopropanol measured at constant contact time were not differential. Therefore, selectivities could not be compared. However, in a separate set of experiments the catalysts were compared at constant conversion (4.73%) in order to determine the selectivities to acetone and propylene (Figure 18). From the activity and selectivity data illustrated in Figures 17 and 18, the acid/base properties of the catalysts can now be assessed.

From Figures 17 and 18 it appears that the ability of the materials to promote a base mediated reaction follows the order:

$$MgO > CsAce/CsNaY > CsAce/CsNaX \simeq CsNaY > CsNaX$$

Unlike MgO and CsAce/CsNaY (Chapters 2 and 3), the propylene formation from CsNaX, CsNaY, and CsAce/CsNaX appears to result from Bronstëd acidity (not reported). Therefore, the acidic character of the materials follows the order:

$$CsNaX > CsAce/CsNaX > CsNaY >> CsAce/CsNaY \simeq MgO$$

4.5.2 Alkylation of Toluene with Methanol

4.5.2.1 Active Base Sites

Considerable evidence has been reported to suggest that base sites are essential for the side chain alkylation of toluene with methanol. The base sites appear to promote: (i) the dehydrogenation of methanol to formaldehyde (2) and (ii) proton abstraction from the methyl group of toluene to form a reactive carbanion intermediate (20). As illustrated in Figures 17 and 18, impregnation of the cesium zeolites results in enhanced dehydrogenation activity and selectivity. For zeolites X and Y, the increase in acetone

yield and selectivity is paralleled by an increase in toluene conversion, although not proportionately (Figure 19). Note that the promotion in toluene conversion resulting from occluded exchange salts in CsNaX has been reported elsewhere as well (8,10). Thus, it appears that a relationship exists between base activity (as defined by acetone production) and the side chain alkylation of toluene. Interestingly, MgO which has been demonstrated here via isopropanol decomposition to possess excellent base activity does not catalyze the alkylation of toluene (Table 5). This too has been reported elsewhere (21) and illustrates that aspects other than active base sites must be important in the side chain alkylation of toluene with methanol.

4.5.2.2 Microporosity

Several authors have suggested that geometric factors may also play an important role for side chain alkylation. It appears that the replacement of sodium ions with cesium not only increases the base properties of the zeolite (Chapter 2 and refs. 22,23) but as suggested by Unland and Freeman (7), serves also to influence the electrostatic forces and geometric constraints within the zeolite pores favoring side chain over ring alkylation. The influence of the cesium cation on toluene adsorption was established further by Sefcik (24) who reported that when toluene was adsorbed into CsNaX and NaX, the rotational frequency (observed by NMR) of toluene located in CsNaX was two orders of magnitude smaller than that recorded for NaX. It was suggested by Sefcik (24) that steric rather than electrostatic forces were responsible for reducing toluene mobility which inturn influences the attack of the methyl group over the aromatic ring. The influence of spatial effects is supported by Garces et al. (4) who demonstrated that cesium salts supported on microporous carbon were just as active for side chain

alkylation as CsNaX. It was noted also that carbon supports with larger pores were not as active.

The adsorption of argon at liquid argon temperatures and at P/Po $< 10^{-3}$ by molecular sieves is generally attributed to microporous adsorption (25,26). Argon was not adsorbed on the MgO used here at $P/P_0 < 10^{-3}$ revealing that no microporosity exists (i.e., < 20Å). Thus, the notion that microporosity may play a role in side chain alkylation of toluene is supported here by argon adsorption and the fact that although MgO and CsAce/CsNaY have similar isopropanol and methanol decomposition (*vide infra*) behavior, toluene conversion is not observed from MgO.

From isopropanol decomposition, CsAce/CsNaY was shown to have considerably more base activity than CsAce/CsNaX (Figures 17 and 18). Moreover, CsAce/CsNaY is known to possess the microporosity suggested to be necessary to influence toluene adsorption. Therefore, one might expect a significant increase in toluene conversion for CsAce/CsNaY over CsAce/CsNaX. However, such is not the case (Table 5).

One possibility why the expected enhancement is not observed is that the impregnation of cesium acetate results in extracrystalline (i.e., external crystal surface) rather than intracrystalline (i.e., internal crystal surface) cesium. Thus, newly formed base sites generated from the decomposition products of cesium acetate would not be in a microporous environment. To determine the location of the decomposition products, superficial-to-bulk analyses were performed. Two samples were prepared. One was CsNaY which was rinsed with a 0.01N cesium acetate after exchange to remove the possibility of any occluded exchange salt yet minimize decationation. The other was CsNaY impregnated by the procedure discussed above at 2.8 wt%. Both sample were calcined in helium at 450°C and submitted for superficial (XPS) and bulk chemical (CA) analyses of silicon and cesium. From Table 7 the superficial-to-bulk ratios (i.e., XPS/CA ratio) were fairly close to unity at 1.15 and 1.22 for the untreated and impregnated

CsNaY zeolite, respectively, suggesting that the cesium is well disperse for both samples. Interestingly, Shannon et al. (27) reported superficial-to-bulk analyses from zeolites to determine whether rhodium was exchanged into the zeolites or remained on the extracrystalline surface after filtration. As evidenced in Table 7 the superficial-to-bulk ratio for zeolite A (1.25 wt% Rh^{3+}) and Y (2.37 wt% Rh^{3+}) was 60 and 1, respectively. These results indicate that rhodium does not exchange into zeolite A (remains extracrystalline) but does in zeolite Y. However, what is more important to this study, the results demonstrate how small surface coverages (1.25 wt% Rh^{3+}) can strongly influence superficial-to-bulk atomic ratios. Thus our superficial-to-bulk data suggest that the decomposition products of cesium acetate are in fact intracrystalline. Therefore, the relatively low activity of CsAce/CsNaY appears to involve the cesium acetate decomposition products in a microporous environment.

4.5.2.3 Stabilization of Formaldehyde

Several authors have suggested that acid sites (Lewis and/or Bronstëd) may interact with the pi electrons of the toluene ring to influence the adsorption of toluene and perhaps increase the acidity of the methyl protons (7,11). It has been suggested also that acid sites may aid in stabilizing formaldehyde and thus suppress its decomposition to CO and H_2. Unland and Freeman (7) demonstrated with infrared spectroscopy that the occlusion of boric acid (most likely in the form of B_2O_3) into the zeolite pores has no apparent influence on the adsorbed toluene yet significantly influences the adsorption of formaldehyde. They concluded that the boron may slow the decomposition of formaldehyde by either (i) providing acidity in the area around the active base sites or (ii) neutralizing strong base sites which may otherwise promote the decomposition of formaldehyde to CO and H_2. These results were supported further by Itoh et al. (11)

who demonstrated using quantum chemical calculations that formaldehyde is far more stable when interacting with an acid site (e.g., H^+) than with a base site (e.g., OH^-).

From the work of Unland and Freeman (7) and Itoh et al. (11), it appears that the decomposition of formaldehyde can be slowed by either direct interaction with available acid sites or neutralization of strong base sites. Noller and Ritter (19) studied the decomposition of methanol over magnesia-silica mixed oxides (i.e., chemical mixtures ranging in composition from 100% SiO_2 to 100% MgO). Acid titration studies using 4-dimethylaminoazobenzene (pK_a = 3.3) suggested that the high silica (10 mol% MgO) and high magnesia (70 mol% MgO) samples had similar acid densities. However, in contrast to the high silica sample, no formaldehyde was observed over the more basic, high magnesia sample. These results may suggest that the rate of formaldehyde decomposition is more strongly influenced by the presence of strong base sites than acid sites.

In Figure 21A, DME and formaldehyde yields during toluene alkylation are shown for both the CsAce/CsNaX and CsAce/CsNaY zeolites as a function of the reaction temperature. For the CsAce/CsNaX zeolite both formaldehyde and DME are observed in the product stream while only trace formaldehyde and DME are observed for CsAce/CsNaY. Furthermore, note that the absence of formaldehyde from CsAce/CsNaY (Figure 21A) is accompanied by a high yield of CO as illustrated in Figure 21B. From the isopropanol decomposition studies (Figure 17 and Chapter 3), CsAce/CsNaY showed virtually no Bronstëd acidity and very high base activity neither of which were suggested to aid in suppressing the rate of formaldehyde decomposition. Moreover, MgO which possesses virtually no Bronstëd acidity and high base activity (Chapters 2 and 3) shows (in agreement with Noller and Ritter (19)) only trace formaldehyde and high CO production as well (Table 5). Therefore, the relatively low

toluene conversions observed for CsAce/CsNaY could result from the rapid decomposition of formaldehyde, i.e., the suggested alkylating agent (2).

The formation of DME from CsAce/CsNaX could be explained by (i) the acidity of the CsAce/CsNaX (demonstrated by isopropanol decomposition to propylene) which may result in an acid catalyzed reaction of methanol to form DME and/or (ii) the reaction of formaldehyde to DME as suggested by Venuto and Landis (28). CsAce/CsNaX possesses moderate base activity and Bronstëd acidity from isopropanol decomposition both of which were suggested to aid in suppressing the decomposition of formaldehyde. Interestingly, Figure 21A shows formaldehyde in the product stream of CsAce/CsNaX.

4.5.3 Alkylation of Other Substrates with Methanol

As discussed above, the deprotonation of the organic substrate to form a reactive carbanion intermediate has been suggested as a key step in the mechanism of side chain alkylation (20). Therefore, it was of interest to establish how substrate C-H bond strength (i.e., acidity) and character (i.e., size and polarity) influenced substrate conversion. From this, reaction diversity can be better assessed. The pK_a values reported for acetone, toluene, methane, and ethane are 20, 35, 40, 42, respectively (30). Note that the pK_a of ethane and methane are only approximate (30). From these values one might expect the order in substrate conversion to follow the order: acetone > toluene > > methane $\simeq$ ethane. From Table 6, it is shown that neither ethane or methane was alkylated. Higher temperatures, e.g., 465°C, did not promote alkylation as well. A report on the alkylation of acetone over Fe^{3+}/MgO (29) suggested that acetone could be alkylated to methylvinylketone over the impregnated zeolites. From Table 6, acetone

was in fact alkylated over both zeolites however the majority of the reacted acetone appeared to form aldol condensation products. Interestingly, the substrate conversions are in fact directly related to the C-H acidity.

In summary, it has been demonstrated that an increase in base character promotes side chain alkylation yet at the expense of formaldehyde decomposition. Thus, to increase alkylation activity it appears that either formaldehdye must be stabilized (as attempted by previous authors) or because of the apparent need for geometric/electronic factors alternate pore structures must be explored.

4.6 *References*

1. Sidorenko, Y. N., Galich, P. N., Gutyrya, V. S., Ilin and I. E. Neimark, Dokl. Akad. Nauk SSSR **173**, 132 (1967).
2. Yashima, T., Sato, K., Hayasaka, T., and Hara, N., *J. Catal.* **26**, 303-312 (1972).
3. Unland, M. L., and Barker, G. E., (Monsanto Co.) U. S. Patent 4,115,424 (September 19, 1978).
4. Garces, J. M., Vrieland, G. E., Bates, S. I., and Scheidt, F. M., *in "Catalysis by Acids and Bases"* (B. Imelik et al., Eds.), Vol. 20, p. 67. Elsevier, Amsterdam, 1985.) p. 51.
5. Zheng, S., Cai, J., and Liu, D., in "Catalysis: Theory to Practice: Proceedings of the 9th International Congress on Catalysis, Calgary, Canada." (M. J. Phillips and M. Ternan, Eds.), Vol. 1, p. 476. The Chemical Institute of Canada, Canada, (1988).
6. Yamaguchi, N., Kobayashi, A., Sodesawa, T., and Nozaki, F., *React. Kinet. Catal. Lett.*, **25**(1-2), 11-15 (1984).
7. Unland, M. L., and Barder, G. E., *in "Catalysis of Organic Reactions,"* (W.R. Moser, Ed.), p.51, Dekker, New York, 1981.
8. Lacroix, C., Deluzarche, A., Kiennemann, and Boy, A., *Zeolites* **4**, 109 (1984).
9. Mamedov, S. N., Khadzhiev, S. N., Alieva, Kh. M., Sarydzhanov, A. A., and Akmedov, E. I., *Kinetika i Kataliz*, **27**(1), 227 (1986).
10. Engelhardt, J., Szanyi, J., and Valyon, J., *J. Catal.* **107**, 296 (1987).
11. Itoh, H., Miyamoto, A., and Murakami, Y., *J. Catal.* **64**, 284 (1980).
12. Gentry, S. J., and Rudham, R., J. Chem. Soc. Faraday Trans. I **70**, 1685 (1974).
13. Jacobs, P. A., Tielen, M., and Uytterhoeven, J. B., *J. Catal.* **50**, 98 (1977).
14. Kim, K. S., Barteau, M. A., and Farneth, W. E., Langmuir **4**, 533 (1988).
15. Parrott, S. L., Rodgers, Jr., J. W., and White, J. M., Appl. Surf. Sci. **1**, 443 (1978).
16. Bowker, M., Petts, R. W., and Waugh, K. C., J. Chem. Soc. Faraday Trans. I **81**, 3073 (1985).
17. Waugh, K. C., Bowker, M., Petts, R. W., Vandervell, H. D., and O'Malley, J., Appl. Catal. **25**, 121 (1986).
18. Bowker, M., Petts, R. W., and Waugh, K. C., J. Catal. **99**, 53 (1986).
19. Noller, H., and Ritter, G., J. Chem. Soc., Faraday Trans. I, **80**, 275 (1984).

20. Tanabe, K., Takahashi, O., and Hattori, H., *React. Kinet. Catal. Lett.* 7(3), 347 (1977).

21. Galich, P. N., Golubchenko, I. T., Gutyrys, V. S.,Ilin, V. G., and Neimark, I. E., *Ukr. Khim. Zh.* 31(11), 1117 (1965).

22. Yashima, T., Suzuki, H., and Hara, N., *J. Catal.* **33**, 486 (1974).

23. Nagy, J. B., Lange, J. -P., Gourge, A. Bodart, P. and Gabelica, Z., *in" Catalysis by Acids and Bases,"* (B. Imelik et al., Eds.) Vol. 20, p. 127. Elsevier, Amsterdam, 1980.

24. Sefcik, M. D., *J. Am. Chem. Soc.*. **101**(8), 2164 (1979).

25. Venero, A. F., and Chiou, J. N., MRS Symp. Proc., **111** 235 (1988).

26. Hathaway, P. E., and Davis M. E., (in preparation).

27. Shannon, R. D., Vedrine, J. C., Naccache, C., and Lefebvre F., *J. Catal.*, **88**, 431 (1984).

28. Venuto, P. B., and Landis, P. S., *Adv. Catal.* **18** , 259 (1968).

29. Ueda, W., Yokoyawa, T., Moro-Oka, Y., and Ikawa, T., *J. Chem. Soc., Chem. Commun.*, 39 (1984).

30. Gordon, A. J., "The Chemist's Companion," John Wiley & Sons, New York, New York, p 63 (1972).

Chapter 5
Overall Conclusions

It was the immediate goal of this work to develop, characterize and apply a catalyst which (i) demonstrates catalytic properties characteristic of solid bases and (ii) provides potential for shape selectivity. The main conclusions from this work are:

5.1 Catalytic Activity

1. The decomposition of cesium acetate impregnated in the CsNaY zeolite results in the generation of a highly active, intracrystalline base site.
2. This highly active base site appears not to form on a similarly prepared CsNaX zeolite or amorphous silica.
3. At 350°C and on a suface area basis, acetone activity for the cesium acetate impregnated CsNaY zeolite is comparable to that found for MgO.

5.2 Nature of the Active Base Stie

1. The nature of the active base site formed by the decomposition of cesium acetate impregnated in CsNaY appears to be a cesium oxide.
2. Point 1 is consistent with results suggesting that the isopropanol dissociatively adsorbs to form an isopropoxide intermediate which may decompose further to form either acetone via α-H^+ abstraction or propylene via β-H^+ abstraction and C-O bond breakage.

From the conclusions of Chapter 2 (Catalytic Activity) and Chapter 3 (Nature of the Active Base Site) it appears that a catalyst now exist which (i) demonstrates activity and

selectivity (as defined by isopropanol decompositon) comparable to MgO, i.e., a solid base, and (ii) provides potential for shape selectivity. It was of interest to apply this novel catalyst to the base catalyzed alkylation of toluene, acetone, ethane, and methane with methanol (Chapter 4). The conclusions from Chapter 4 are:

5.3 Alkylation with Methanol

1. The acid/base properties (defined by isopropanol decomposition) of the impregnated zeolites measured at 425°C are consistent with those obtained at 350°C.
2. Toluene alkylation is promoted when CsNaY and CsNaX are impregnated with cesium acetate suggesting that base sites are essential for side chain alkylation.
3. The promotion in base character of the impregnated CsNaY zeolite appears also to enhance the decomposition of the formaldehyde, i.e., the suggested alkylating agent.
4. An optimum conversion may exist for the faujasite-type catalysts, i.e., increasing the base character of the zeolite may promote toluene conversion, yet it appears also to promote the formaldehyde decomposition.
5. Although MgO and cesium acetate impregnated CsNaY have similar base properties, toluene is not alkylated by MgO suggesting that geometric/electronic factors may be important for side chain alkylation.
6. The alkylation of acetone and toluene over ethane and methane suggests that the ability of the substrate to stabilize a reactive carbanion intermediate is vital in base catalyzed alkylation with methanol.
7. Most of the reacting acetone forms what appears to be base catalyzed, aldol condensation products and thus may compete with methanol alkylation.

Chapter 6

Future Directions

This chapter adresses experiments which were not disscussed and those which should be considered for future work.

6.1 Experiments Not Disscussed:

6.1.1 Impregnation of Ultrastable Y

Cesium exchanged, ultra stable Y (USY) impregnated with cesium acetate showed no isopropanol decomposition. This is consistant with the impregnation of the silica gel with cesium acetate which also showed no isopropanol decomposition. These results coupled with the low acetone activity of the impregnated CsNaX zeolite suggest that the

Si/Al ratio may play an active role in generating cesium oxide - the suggested base site suspect in the promotion of acetone formation.

6.1.2 Alkylation with Ethanol

In the alkyaltion of toluene, methanol was substituted for ethanol. This experiment was geared towards understanding how the decomposition of the formaldehyde influenced the conversion of toluene. It was postulated that ethanal might be more stable than formaldehyde and thus promote the conversion of toluene. Interestingly, no propylbenzene or allylbenzene was observed. However, trace amounts of styrene and ethylbenzene were observed. It is believed that this negative result could in fact shed more light towards understanding the mechanism for alkylation which in turn may improve toluene conversion to styrene.

6.1.3 Shape Selectivity

It was of interest to establish shape selectivity with a base catalyzed reaction. The catalysts chosen were CsAce/CsNaY (possible shape selectivity) and MgO (no shape selectivity). The reactions chosen were the dehydrogenation of 1-hexanol to hexanal (little steric hindrance with MgO or zeolite) and the dehydrogenation of cyclooctanemethanol to cyclooctanecarboxaldehyde (possible steric hindrance with the zeolite). Note that both reactants are primary alcohols. The experimental conditions were as follows: at a 1:1 ratio of hexanol-to-cyclooct., the reactants were diluted in cyclohexane (95 mole percent diluent), the W/F was 15.2 X 10^3 m^2 • h • (moles hexanol

+ cyclooct.)$^{-1}$, the flowrates of helium, hexanol, and cyclooct. were 100, 0.15, and 0.15 cc(STP)/min, respectively, and the reaction temperature was varied from 300°C to 400°C.

For MgO (125 m^2/g), both alcohols reacted to their respective aldehydes (>97% selectivity), as expected, and the conversion increased with temperature. By replacing MgO with CsAce/CsNaY (492 m^2/g), one hopes to observed the dehyrogenation of the linear alcohol with little or no dehydrogenation of the cyclic alcohol (except perhaps extracrystalline reactivity). For CsAce/CsNaY, the linear alcohol reacted to the aldehyde (hexanal), however, the cyclic alcohol reacted as well. The reaction products from the cyclic alcohol contained little aldehyde (cyclooctanecarboxaldehyde) but contained considerable amounts of what appears to be isomerization products.

6.2 Future Directions

An area to pursue in this work is to establish the influence of the Si/Al ratio, i.e., the inability of CsNaX, silica gel, and Cs-USY to promote acetone formation upon cesium acetate decompositon. It would therefore seem logical to (i) synthesize faujasite-type zeolites which vary in Si/Al ratios from ~1 to ~6, (ii) exchange these zeolites to the cesium form, (iii) impregnate these zeolites with cesium acetate at a constant loading, and (iv) expose these zeolites to isopropanol to obtain their respective rates of acetone and propylene formation. It may be of interest also to complement the isopropanol results with ^{133}Cs MAS-NMR. Recently [1] it was shown that ^{133}Cs MAS-NMR per-

[1] Chu, P. J., Gerstein, B. C. Sheffer, G. R., and King, T. S., J. Catal., 115 194 (1989).

formed on CsCl, Cs_2CO_3, CsOH, CsCHO, and $CsNO_3$ provided a viable method for distinguishing cesium in different environments. It may be of interest to (i) do ^{133}Cs MAS-NMR on the untreated, cesium exchanged zeolites (varing in Si/Al ratio), (ii) impregnate these zeolites with cesium acetate and repeat the NMR experiments, and (iii) compare the respective spectra in hopes of observing peaks (as defined by standards, e.g., Cs_2O) which result from the decomposition products of the cesium acetate. This may not only shed more light on the nature of the active base site formed by the decomposition of the acetate, but may also reveal information concerning the influence of the Si/Al ratio, i.e., the formation of cesium silicates or cesium aluminates.

Once the influence of the Si/Al ratio is determined it may be of interest to expand the technique of acetate impregnation and decomposition to zeolites which differ in topology. Of greatest importance would be medium pore zeolites (e.g., ZSM-5, ZSM-11, ZSM-48) which may provide greater promise for shape selectivity.

The vita has been removed from the scanned document